

Crack Systems Analysis of the McCartys Flow, New Mexico, USA

Charles Wise
May 2014

Senior Thesis

Submitted in partial fulfillment of the requirements
for the Bachelor of Arts degree in Earth Science

Advisor, Professor Jeffrey R. Walker

Table of Contents

Acknowledgements.....	3
Abstract.....	5
Chapter One: Introduction to Basalt, Basaltic Lava, and Inflation.....	6
Chapter Two: The Zuni-Bandera Volcanic Field	13
Chapter Three: McCartys Flow Field Work	22
Chapter Four: Analysis of the Crack Classification Model and DGPS Data Sets.....	26
Chapter Five: Applications to Mars	41
Chapter Six: Conclusions.....	44
References	47
Appendix.....	50

Acknowledgements

Firstly, I want to thank everyone who was part of the Keck Geology Consortium Martian Pahoehoe Lava project for funding and supporting this research: Professor Andrew P. de Wet of Franklin & Marshall College for leading a great project and helping me narrow my focus, Dr. Christopher Hamilton of the University of Arizona and Dr. W. Brent Garry of the NASA-Goddard Spaceflight Center for working with me in the field on the McCartys Flow, and Dr. Jacob Bleacher of the NASA-Goddard Spaceflight Center for all the encouragement and help in the field. My colleagues who worked in the field with me: Jessica McHale of Mt. Holyoke College, Megan Switzer of Colgate University, and Susan Konkol of the University of Nevada who worked on the McCartys Flow with me, as well as Ryan Samuels of Franklin & Marshall College and Hester von Meerscheidt of Boise State University who worked on the Bandera Flow. You were the best team I could have ever asked to work with.

At Vassar College, I want to thank Professor Jeffrey R. Walker for agreeing to serve as my advisor on this project and giving me valuable feedback on my drafts, Professor Kirsten Menking, who has tirelessly served as my advisor for the past four years, and Professor Jill Schneiderman for all the positive encouragement and feedback. It was good to know that even in my darkest of moments, you all still believed in me.

I would like to thank my parents, Tracy Wise and Margaret Braae, for their unwavering support of my educational endeavors throughout my life and for teaching me that what matters most is how well you walk through the fire.

Finally, I would like to thank Geneva Ruppert for always believing in me and for being there whenever I felt the walls closing in around me. Without you, I never would have made it. Thanks, love.

Dedicated to Chase Pinkham,
one of the best men I ever knew.

Rest in peace, my friend.

Abstract

The McCartys Flow is a 3.9-ka vesicular porphyritic basalt lava flow in the Zuni-Bandera Volcanic Field (ZBVF) near Grants, New Mexico. The Lava Falls area on the southern part of the flow is dominated by pahoehoe sheet flows. Topographic features such as plateaus, depressions, monoclines, escarpments, and en-echelon cracks are interpreted as being formed by inflation. Using detailed observations of the Lava Falls area and differential GPS (DGPS) transects, the crack systems of these topographic features were constrained to three different crack patterns. Particular crack patterns were constrained to flow margins and depressions. Analysis of crustal and structural widths along transects indicates that up-swelling was likely responsible for crack formation, though this extension was not necessarily constant. A model of emplacement is suggested to explain the progression of inflation along the flow in a plateau-like fashion of decreasing elevation from the McCartys vent. Finally, the results of the McCartys Flow fieldwork and analysis are discussed as a possible approach examining suspected inflation features in the Elysium Volcanic Province on Mars.

Chapter One

Introduction to Basalt, Basaltic Lava, and Inflation

Basalt is an extrusive, igneous rock, and is the most common rock type at the surface of the Earth and on other terrestrial planets. Basaltic lavas consist of two main groups: (1) tholeiitic or subalkaline, which are poor in trace elements and typical of ocean crust and flood basalts, and (2) alkaline basalts, which contain higher levels of potassium, sodium, and other trace elements and occur more commonly in smaller terrestrial and oceanic volcanoes (Schmincke 2004). In regards to terrestrial basaltic lavas, the Hawaiian terms a’ā and pahoehoe are used to describe the



Figure 1 – The two kinds of subaerial basaltic lava flows. (Top) A thick, blocky a’ā flow. (Bottom) The smooth, ropey texture of a pahoehoe flow. U.S. Geological Survey

two principal types of subaerial basaltic lava flows. A’ā refers to rough, thick, blocky lava indicating tearing apart and strong driving forces (Figure 1, top). Pahoehoe refers to smooth, ropey, billowy lava indicating more fluid effusion (Figure 1, bottom). Once lava flows have solidified, more descriptive terms pertaining to their physical appearance such as “ball and groove texture” or “lineated” may be used. The ratio between driving and resisting forces determines the texture type of the lava (either a’ā or pahoehoe). Hawaiian a’ā flows are generally fed by lava with a Bingham rheology (a rigid body at low stress, flows as a viscous fluid at high stress) possessing a significant

yield strength that must be overcome before they flow. In contrast, Hawaiian pahoehoe flows are mostly fed by lava with an approximate Newtonian rheology (low yield strength, constant viscosity affected only by changes in temperature and pressure). Typically, flows transition from pahoehoe to a'a as they flow away from a vent, but a'a to pahoehoe transitions have also been observed in channelized a'a flows that advance from steeper slopes onto flatter terrain (Hon et al. 2003).

Pahoehoe flows dominate terrestrial basaltic lavas on Earth both in terms of areal coverage and volume (Self et al. 1998). Several extraterrestrial flows also seem to be pahoehoe. Pahoehoe flow emplacement begins with the formation of pahoehoe toes at the leading edge of thin fluid lava sheets. These sheets (20-30 cm thick) form due to low yield strengths (near-Newtonian rheology) and low viscosity of the lava, as observed in tholeiitic Hawaiian pahoehoe flows (Hon et al. 1994). As the outermost layer of lava rapidly cools, it forms a thin skin (<1-2 mm thick) around the sheet that retains the incoming lava, deviating from Newtonian behavior. Internal pressure deforms the skin plastically, allowing it to swell into toes at the flow front that rupture to form neighboring toes (Figure 2) (Hon et al. 1994). Pahoehoe toe development is strongly controlled by topography. Hon et al. (1994) observed that pahoehoe toes that formed on relatively flat, gently sloping surfaces often impinged on the growth of neighboring toes before a solid crust could completely form, allowing toes to coalesce to form a continuous liquid lava core with a single overlying crustal layer. These features are called lobes, the smallest most coherent packages of lava (Figure 2) (Self et al. 1998). As long as the supply rate of lava to the lobe is sufficiently high, new low-strength, thin crust is produced at the flow front, allowing the lobe to advance (Hoblitt et al. 2012). Advancing pahoehoe lobes observed in Hawaii by Self et al. (1998) were typically 20-50 cm thick, 20-300 cm wide, and 0.5-5 m long. Lobe emplacement

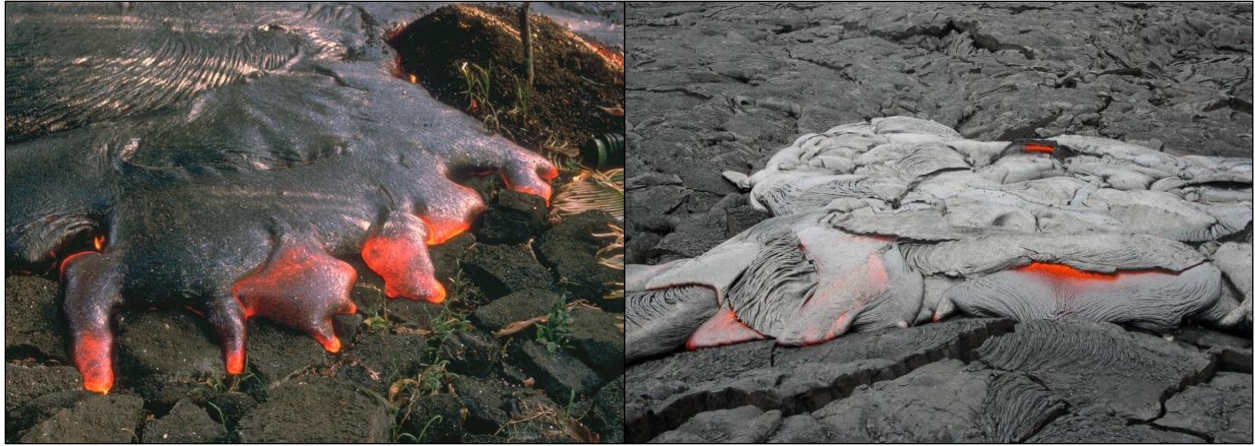


Figure 2 – (Left) A thin, fluid lava sheet with pahoehoe toes swelling and forming at the leading edge. (Right) A group of pahoehoe lobes, which form from coalescing pahoehoe toes that form a single, continuous liquid core contained by a thin crust. U.S. Geological Survey

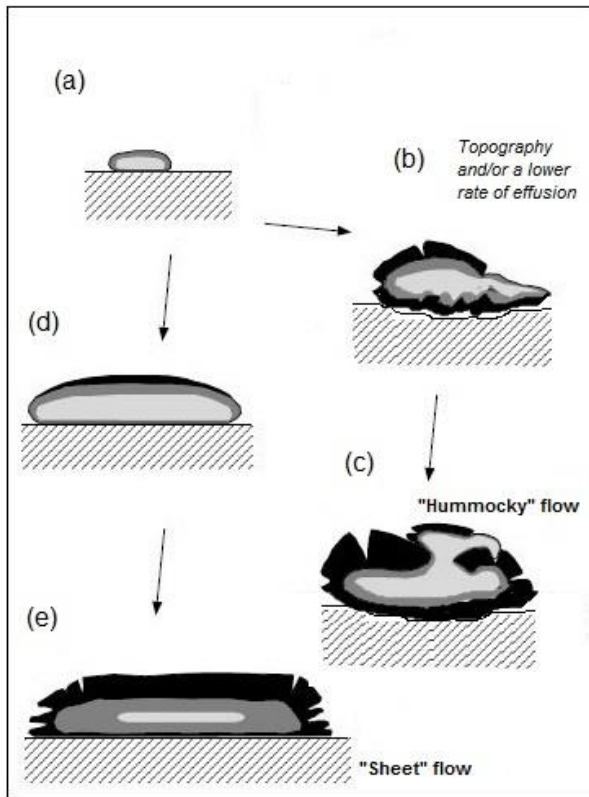


Figure 3 – Cartoon cross section of sheet flow and hummocky flow formation. A pahoehoe lobe (a) that is discontinuously emplaced on a slope or rough topography (b) will generally produce a hummocky pahoehoe flow with positive topographic features along the flow surface called tumuli (c). Conversely, pahoehoe lobes that are rapidly emplaced on smooth, shallow slopes (d) generally produced smooth, sheet flows (e). Adapted from Self et al. (1998)

and development is controlled by factors such as effusion rate and topography. Self et al. (1998) observed that rapid, continuous emplacement of lobes over smooth surfaces with shallow slopes generally produced pahoehoe flows dominated by sheet-like lobes, or “sheet” flows (Figure 3). In contrast, discontinuous and relatively slow emplacement over rougher surfaces with steeper slopes generally produced “hummocky” pahoehoe flows with positive topographic features, referred to as tumuli (Figure 3) (Walker 1991). Lava pathways in hummocky flows have many dead ends where lava cannot flow, creating discrete lava tubes

that contribute to the irregular flow thickness. Sheet flows, in contrast, have a continuous body of liquid lava across the entire flow width, however, should a sheet flow remain active long enough for parts of the sheet to cool shut, the resulting irregularities in flow thickness will also produce preferred pathways and subsequently hummocky pahoehoe flow. The larger and thicker the flow, the more likely it is to be sheet-like, whereas thinner flows are more vulnerable to the development of narrow, preferred pathways and are thus more likely to be hummocky. Both sheet and hummocky pahoehoe flows may grow into even larger flow fields or lava plateaus several meters high, hundreds or thousands of meters wide, and ranging from hundreds of meters to several tens of kilometers in length (Self et al. 1998).

Fink & Fletcher (1978) characterize pahoehoe flows as having a smooth, flexible skin of cooler lava that forms ropes and other small-scale features when deformed by motion indicating different lava flow facies. Keszthelyi (2013) proposes dividing the products of mafic volcanism into three sets of morphologic facies: near-vent, transport, and flow front. Near-vent facies begin as widespread pyroclastic fallout, progressing to shelly pahoehoe and possible lava ponds before edifices around the vent start to collapse, forming small pits. Transport facies initially are fluid lava carried in a broad sheet with an interconnected interior that soon develops preferred pathways, channels, or tubes, which in the long term may become well-established. At the flow front, the facies follow a pattern of either a'a or pahoehoe surface texture formation depending on the ratio between driving and resisting forces, focusing the advance along distinct lobes fed by interconnected transport pathways and in later stages often featuring secondary breakouts after the flow has stagnated.

The mechanism responsible for producing flow fields and plateaus to the dimensions described by Self et al. (1998) is inflation, first characterized by Hon et al. in their landmark

1994 paper. As pahoehoe lobes spread away from their point of outbreak, they begin to slow their advance and form a crust capable of retaining incoming lava (Figure 4a, b). When the tensile strength of the flow is exceeded, the inflated front ruptures and a new lobe forms from the outbreak. The process repeats itself to produce successive inflated lobes that are all linked together to form a single flow. Because these successive lobes are all hydrostatically interconnected, the hydrostatic pressure is distributed equally throughout the liquid lava core of the flow, resulting in relatively uniform uplift of the solidified crust (Figure 4b, c, d) (Hon et al. 1994). The crustal structure model of inflated pahoehoe sheet flows developed by Hon et al. (1994) divides the upper crust of the flow into three distinct layers (Figure 5). The lowest is a viscous layer that forms when lava immediately adjacent to the solidifying crust begins to cool, effectively becoming part of the crust itself. This layer serves as a thin boundary between the active liquid core of the flow and

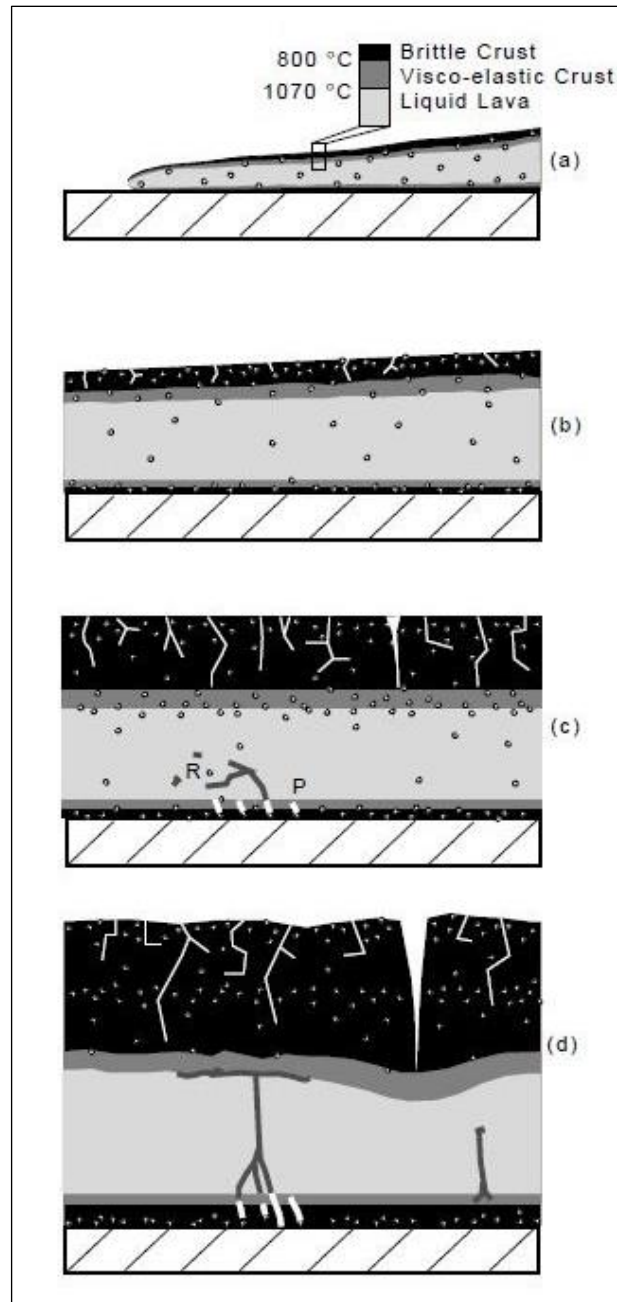


Figure 4 - Cartoon cross section of the development of an inflated pahoehoe flow. (a) An advancing lobe forms a brittle crust capable of retaining incoming lava and (b) begins to inflate, thickening the liquid core and the brittle outer crust. (c) As inflation continues, a new breakout depressurizes the flow and leads to a pulse of vesiculation in the form of vesicular silicic residuum (R) and pipe vesicles (P). (d) Eventually the flow stagnates and inflation ceases. The vesicular residuum (R) is able to rise through the now stagnant lava forming horizontal vesicular sheets at the base of the viscoelastic layer. Note that this particular figure omits the viscous layer as described by Hon et al. (1994). Adapted from Self et al. (1998)

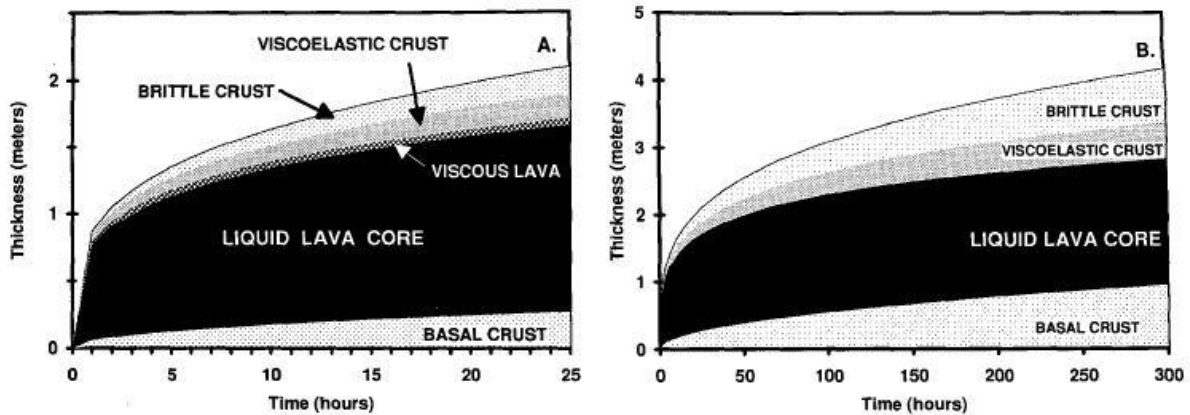


Figure 5 - A model of crustal structure development (A) after 25 hours and (B) after 300 hours by Hon et al. (1994) based on quantitative analysis performed on an inflated sheet flow on the 13 April 1990. The boundary between the brittle crust and the viscoelastic layer marks the 800 °C isotherm, and the boundary between the viscoelastic layer and the viscous layer marks the 1070 °C. Note the decrease over time in percentage of the upper crust that the viscoelastic layer occupies and the simultaneous thickening of the liquid lava core as the flow is inflated over time. Adapted from Hon et al. (1994)

the overlying solidified crust, stabilizing at a thickness of about 0.05 m. The minimum temperature of this layer is 1070 °C, which marks the boundary where actual crust begins to form (Figure 5). The middle layer is a solidified crust between 800-1070 °C that behaves viscoelastically and therefore is assumed to largely govern the tensile strength of the sheet flow. Below 800 °C, the viscoelastic layer behaves rheologically like a solid, but within the aforementioned temperature range it behaves like silly putty; slow stress causes stretching, but fast stress causes breaking and snapping. The viscoelastic layer initially makes up almost 100% of the pahoehoe crust, but decreases over time before stabilizing at about 40% of crustal thickness at 100 hours after flow formation. Finally, the top layer is the outer, cooler crust that fractures in a brittle fashion during flow inflation and thickens as it cools over time (Figure 5).

Self et al. (1998) observed that during inflation, surface topography often becomes inverted. Topographic lows in the underlying geography will form tumuli features across the flow, while topographic highs will produce depressions (Figure 6). Walker (1991) called these depressions “lava-rise pits” because he interpreted them as generally being formed by the elevation of the lava around them, as opposed to previous interpretations that attributed them to

collapse or subsidence. While technically correct, the term “inflation pit” is used instead in this paper.

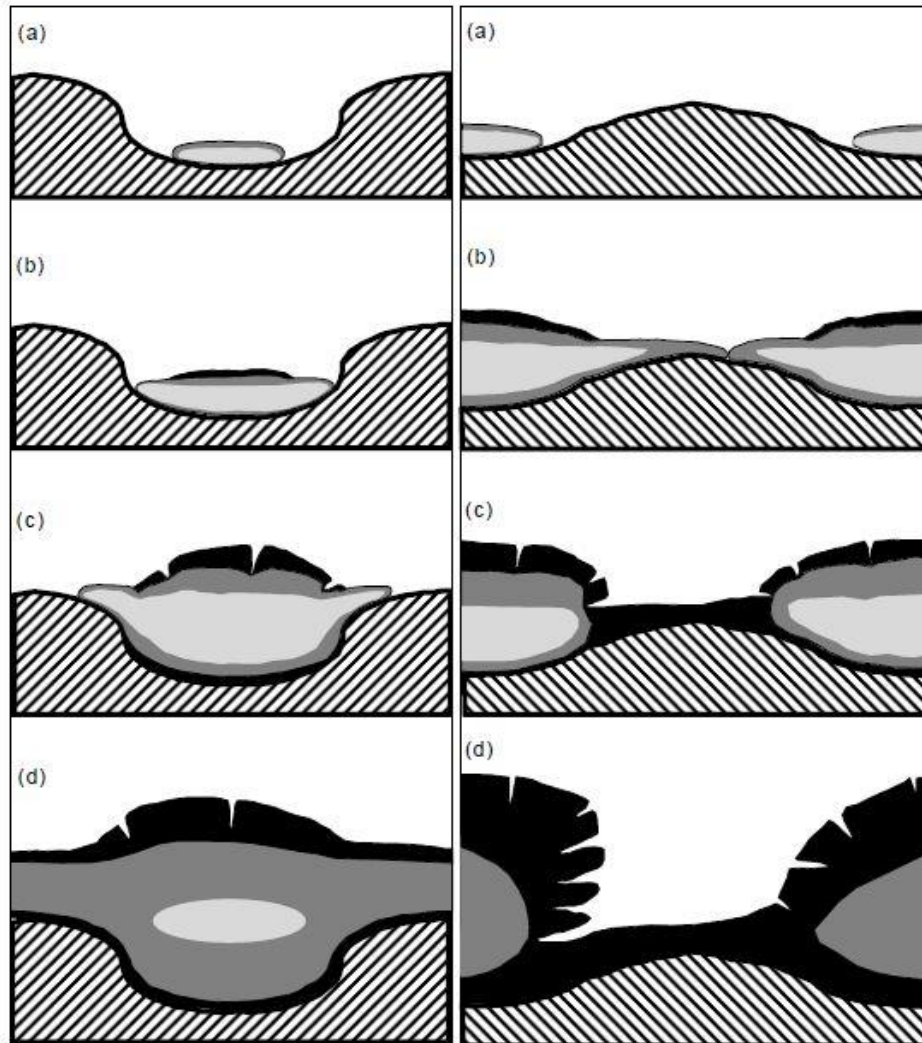


Figure 6 – Cartoon cross sections of the development of tumuli (left) and inflation pits (right) in inflating pahoehoe flows. (a) Initial pahoehoe lobes are confined to low areas. (b, c) As the flows advance, they inflate and spread laterally through breakouts, eventually covering earlier high ground. (d) A continuous flow forms over the original high points in the case of tumuli (left), or a depression forms over the original high point in the case of inflation pits (right). *Adapted from Self et al. (1998)*

Chapter Two:

The Zuni-Bandera Volcanic Field

The Zuni-Bandera Volcanic Field (ZBVF) is a volcanic field located to the south of the town Grants, New Mexico, within the El Malpais National Monument. The ZBVF consists of a large number of basaltic lava flows, containing both a'a and pahoehoe lavas and a lava-tube system, and cinder cones. The field lies near the center of the Jemez lineament, a linear feature running from central Arizona to west-central New Mexico displaying localized late-Cenozoic basaltic volcanism containing zones of crustal weakness that penetrate deeply into the lithosphere. The ZBVF occurs at one of these sites of crustal weakness on a transition zone between the Colorado Plateau and the Rio Grande Rift province. The basaltic lavas of the field appear to be mantle-derived melts resulting from decompression with the transition away from the Colorado Plateau (Laughlin et al. 1982). Geochemically, the ZBVF contains both tholeiitic and alkaline basalts (Dunbar & Phillips, 2004) consisting primarily of basalt (40-50 percent silica), rhyolite (more silicic, at surface), and at a deeper level granites and gabbros. The volcanism of the field is described as "plains volcanism" or "dispersed volcanism", owing to the presence of at least 100 vents in the field that formed numerous smaller pathways for magma to reach the surface and the presence of many features of Hawaiian-style volcanism (Walker 1991; Hon et al. 1994) such as pahoehoe flow patterns, wedge-shaped cracks, flow depressions, and tumuli. Eruptions have been occurring at the field for over 1 Ma in approximately 30-ka intervals (Laughlin et al. 1993).

From 09-15 July 2013 investigations were undertaken on two solidified lava flows within the ZBVF as part of the 2013 Keck Geology Consortium Martian Pahoehoe Lava project. The project was led by Professor Andrew P. de Wet (Franklin & Marshall College), Dr. Christopher

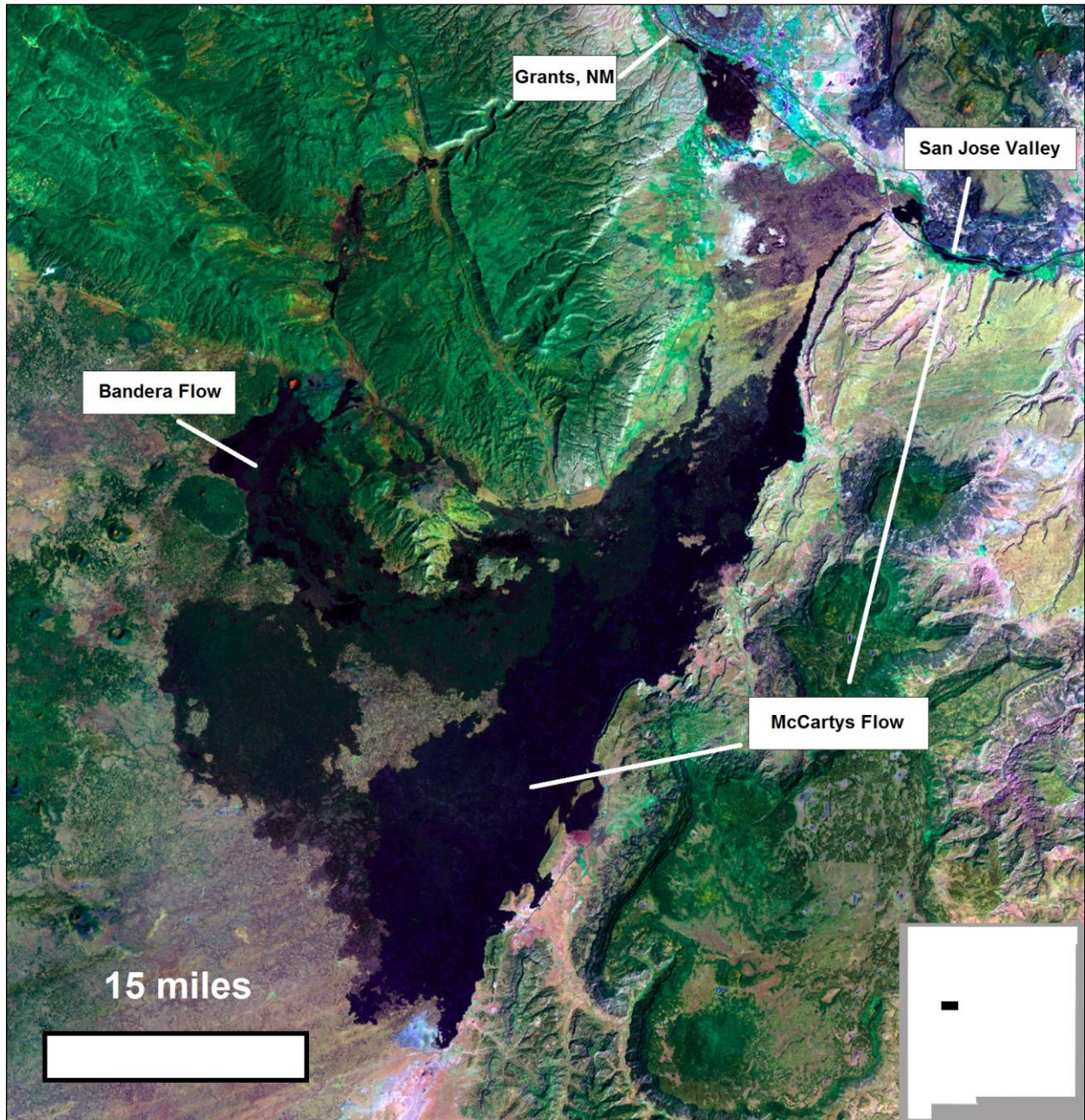


Figure 7 - The Zuni-Bandera Volcanic Field near Grants, New Mexico. The lava flows are indicated by the black, grey, and dark brown colors. The two main sites of the Keck investigations were the Bandera Flow and the McCartys Flow. *Adapted from Landsat image courtesy of the New Mexico Bureau of Geology and Mineral Resources*

Hamilton (University of Arizona), Dr. Jacob Bleacher (NASA-Goddard Space Flight Center) and Dr. W. Brent Garry (NASA-Goddard Space Flight Center). The two solidified lava flows within the Zuni-Bandera field that were closely investigated during field work were the Bandera Flow and the McCartys Flow (Figure 7 and Figure 8).

The Keck team consisted of six students including myself: Jessica McHale (Mt. Holyoke College), Susan Konkol (University of Nevada), Megan Switzer (Colgate University), Hester von Meerscheidt (Boise State University), and Ryan Samuels (Franklin & Marshall College). Von Meerscheidt and Samuels focused their research on the Bandera Flow under the direction of Dr. Bleacher and Professor de Wet. McHale, Konkol, Switzer and I focused our research on the McCartys Flow under the direction of Dr. Hamilton and Dr. Garry. McHale subsequently modeled the crack systems of the flow using PEG hydrogel simulations. Konkol examined a series of depressions in the southern portion of the flow. Switzer collected field samples from different levels of the inflated flow and performed a geochemical analysis of their chemical

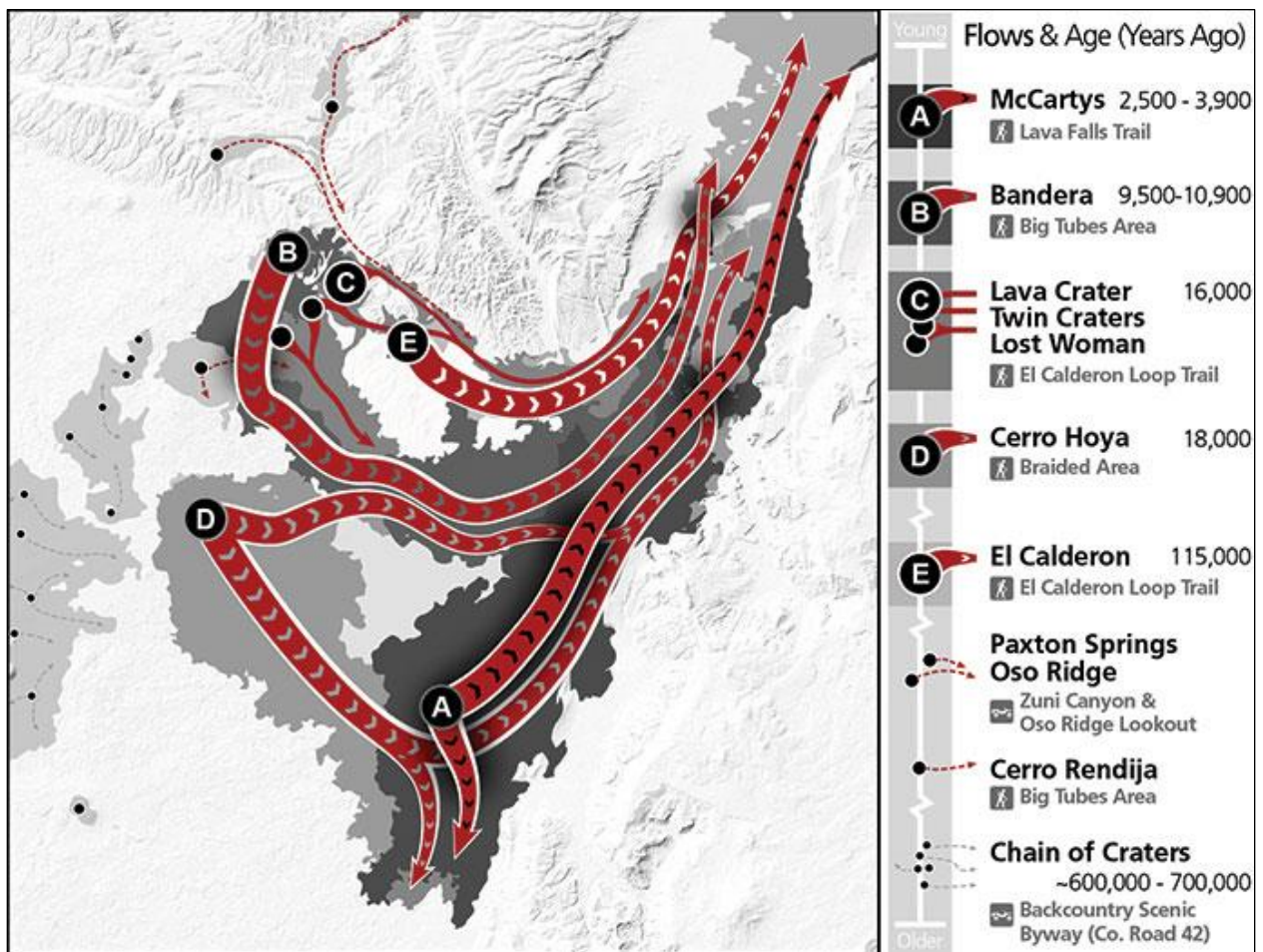


Figure 8 - Map of the major lava flows of the Zuni-Bandera Volcanic Field and their flow directions. Field work for this particular project took place on the southern portion of the McCartys Flow (A). No scale was provided for this map in the original documentation. North is up. *National Park Service*

make-up. My research analyzed the crack systems of the McCartys flow as indicators of inflation and flow emplacement history. 09 July was spent working on the Bandera Flow and 10-15 July was spent working on the McCartys Flow, primarily near Lava Falls.

The McCartys Flow is the youngest basaltic lava flow on the ZBVF. Its source is a low shield volcano located at the center of the flow (approximately 25 miles south of the intersection of Interstate Highway 40 and New Mexico Highway 117) (Laughlin et al. 1993). Most of the lava flowed northward, following a pre-existing drainage, reaching as far as the San Jose Valley, as well as southward for about 6 miles, covering an area of 119 sq. miles (Figure 7) (Nichols 1946). The flow is typically vesicular porphyritic basalt dominated by large plagioclase phenocrysts within 4 km of the source and olivine phenocrysts at greater distances (Carden & Laughlin 1974; Laughlin et al. 1993). Of particular interest is the Lava Falls area, located on the southern edge of the McCartys Flow, which is dominated by pahoehoe flows. Topographic features here such as plateaus, (containing several concentric and elongate depressions), monoclines, escarpments, and deep cracks have been interpreted as formed by inflation of pahoehoe sheet flows (Mabery et al. 1999; Hon et al. 1994).

The McCartys Flow was first thoroughly investigated by Nichols (1946). Nichols's observations led him to date the flow at approximately 1000 years old and interpret the crack systems formed on the flow as the result of crustal expansion due to uplift during construction of the plateau and thermal contraction as the lava of the flow cooled. Nichols also attributed the series of depressions on the southwest of the flow (Figure 10, top) as being the collapsed roofs of lava tunnels, whose distribution indicated either a partial collapse of one large tunnel or several smaller ones. Laughlin et al. (1993) in their roadside geology guide of El Malpais noted that the flow overlies older basalts of the ZBVF and alluvium and dated the flow using both charcoal

from baked soil and the ^3He method for surface flow samples, producing average ages of 3160-3200 and 2450 years old, respectively. The groundbreaking work done on pahoehoe flows by Walker (1991) and Hon et al. (1994) re-interpreted Nichol's findings by attributing the formation of the crack systems, monoclines, plateaus, and depressions on pahoehoe sheet flows to inflation. Mabery et al. (1999), in their guidebook to the El Malpais National Monument, also attribute these features to inflation, citing Hon et al. (1994) as the source of their interpretations. Though Dunbar & Phillips (2004) do not explicitly say if inflation is the cause of the features observed within the ZBVF, they state that the field exhibits a number of features characteristic of Hawaiian-style volcanism and estimate the average cosmogenic ^{36}Cl age for the McCartys Flow to be 3.9 ± 1.2 ka, currently the oldest accepted date of the flow.

It should be noted that the terminology in regards to "cracks" varies from "lava-inflation cleft" (Walker 1991) to "crack" (Hon et al. 1994) and to "rift" (Hoblitt et al. 2012). The term crack is used in the context of this paper because it was used by our research team both in the field and during subsequent data analysis.

Crack systems on pahoehoe flows serve as indicators of inflation in a number of ways. Walker (1991), describing what he termed "lava-rise plateaus" (inflated pahoehoe sheet flows), observed plateau edges circumscribed by steep escarpments cut by sub-horizontal cracks or marked by tilted crustal plates. Hon et al. (1994) confirmed Walker's observations by describing the flat upper surfaces of inflated sheet flows as bound by monoclinial flexures dipping between 10° - 80° , with upper hinges of the flexures marked by en-echelon cracks as deep as 1-2 m. Hoblitt et al. (2012) confirmed that cracks from inflation were best developed at flow margins because the viscoelastic layer is thinnest there and more susceptible to extension. They

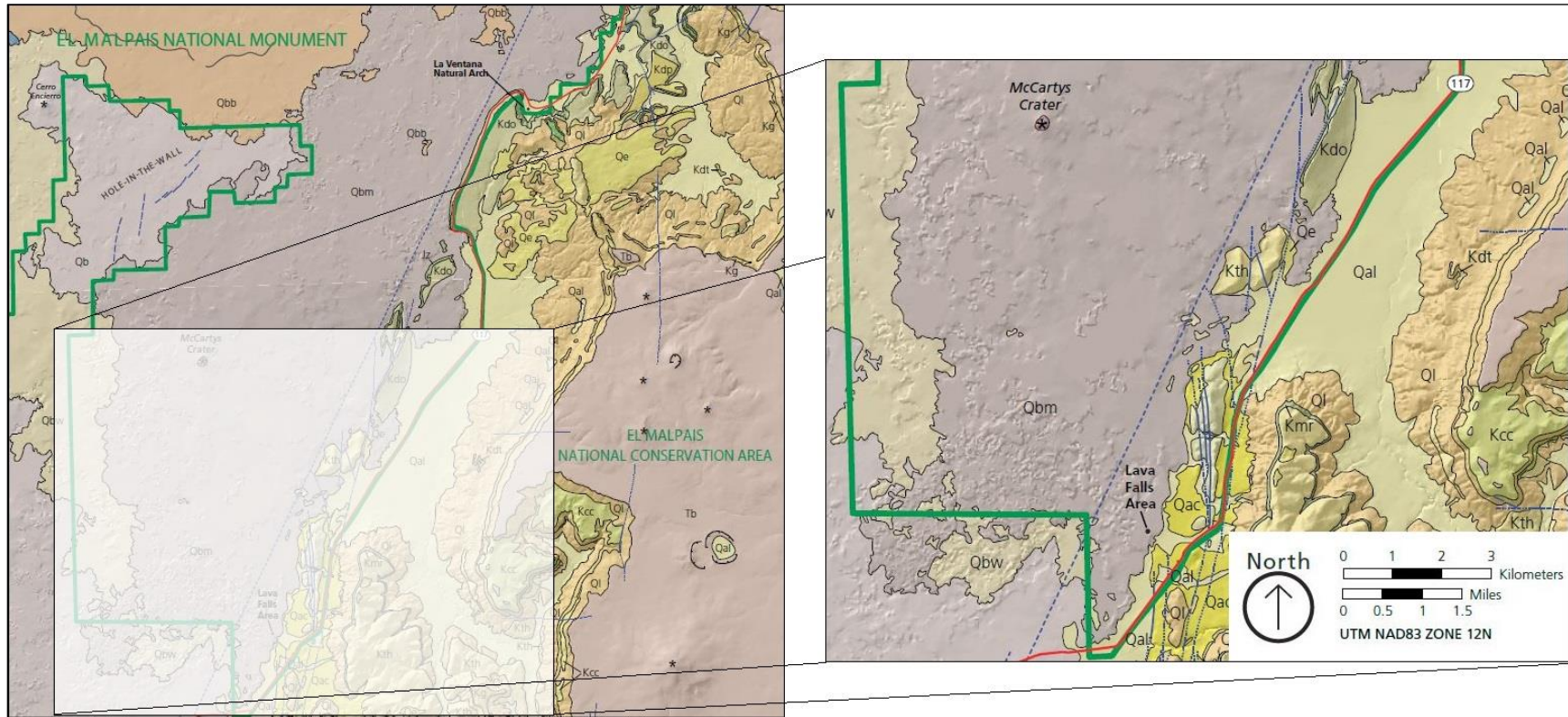


Figure 9 - Modified geologic map showing the location of the Lava Falls area of the McCarty's Flow within the southern area of El Malpais National Monument. Kcc - Crevasse Canyon Formation. Kdo - Mancos shale, Dakota sandstone. Kdt - Dakota sandstone. Kmr - Mancos shale. Kth - Tres Hermanos sandstone. Qac - alluvium, colluvium, and soil. Qal - alluvium. Qbm - McCarty's Flow. Qbw - Hoya de Cibola flows. Qe - eolian deposits. Ql - landslide deposits. The green lines are the National Monument boundaries and the red line is Route 117 coming down from Grants. A larger view of the Lava Falls area can be seen in Figure 10. Adapted from the National Park Service

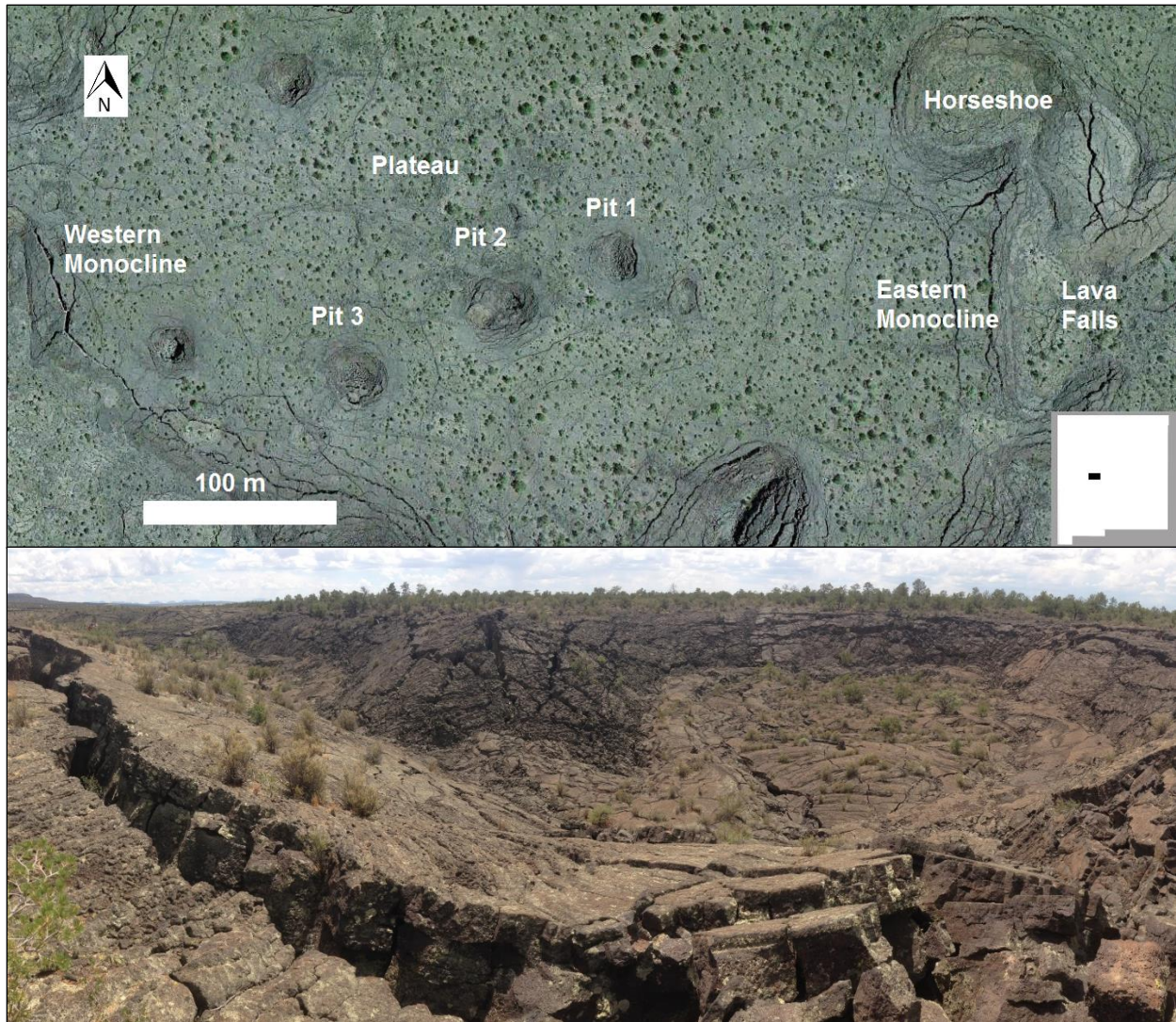


Figure 10 - (Top) The Lava Falls area on the southern tip of the McCartys Flow with major areas of investigation labeled. Adapted from Google Earth (Bottom) The Horseshoe area of Lava Falls, viewed from the southwest. Jacob Bleacher

described two main styles of cracking: a dominant style characterized by outward-dipping slabs, similar to the observations of Walker (1991) and (Figure 11), and a subordinate style characterized by vertical scarps. Uplift of thicker, brittle crust in young pahoehoe flows is also responsible for large crack systems bounding sheet-flow margins and networks of smaller cracks scattered across the flow surface (Hon et al. 1994). Comparison of the total line length across the upper surface of the sheet flow minus the cumulative crack widths to a horizontal base line should demonstrate at least 1% of extension from the cracking (Figure 12A). Walker (1991) also

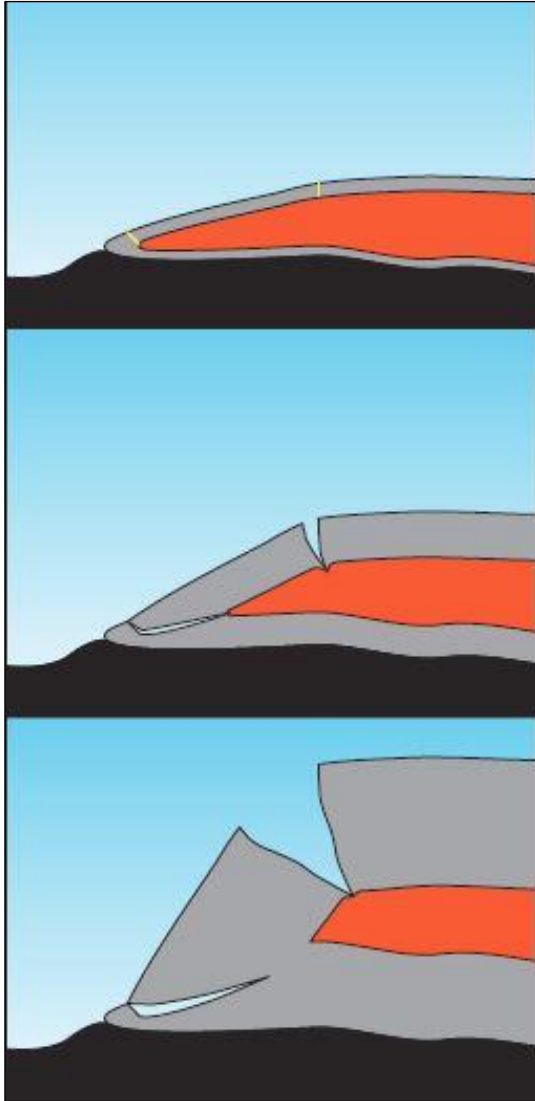


Figure 11 – Cartoon cross section of tilted slab cracking on the margins of sheet flows. Grey indicates brittle lava; orange the viscoelastic layer; and black pre-existing surface. As the slab rotates, one crack propagates inward and upward near the base while a second crack propagates downward and inward from the top of the slab (middle). As inflation continues, the lower crack becomes inactive but the upper crack continues to tilt (bottom). Adapted from Hoblitt et al. (2012)

measured crack widths across profiles of tumuli to determine whether the cracking present in these profiles was the result of lateral pressure transmitted through a rigid crust (like pressure ridges in sea ice) or from simple up-swelling, likely caused by inflation. According to the criterion developed by Walker (1991), cracking is due to up-swelling if the total crustal width of the structure (crustal width measurement in Figure 12B) is equal to or less than the width of the structure (tumulus width measurement in Figure 12B). Finally, depressions observed in inflated pahoehoe flows also exhibit particular cracking patterns indicating that they are inflation pits as opposed to collapse pits or lava tubes. Walker (1991) characterized the edges of what he termed “lava-rise pits” (inflation pits) as identical to the edges of “lava-rises” (inflation rises/plateaus), noting that the surface crust often formed an overhang around the top and crustal plates could

be tilted down into the pit bottom. Hon et al. (1994) observed that where sheet flows surrounded pre-existing topographic highs, vertical uplift scarps were formed as the lava inflated around the

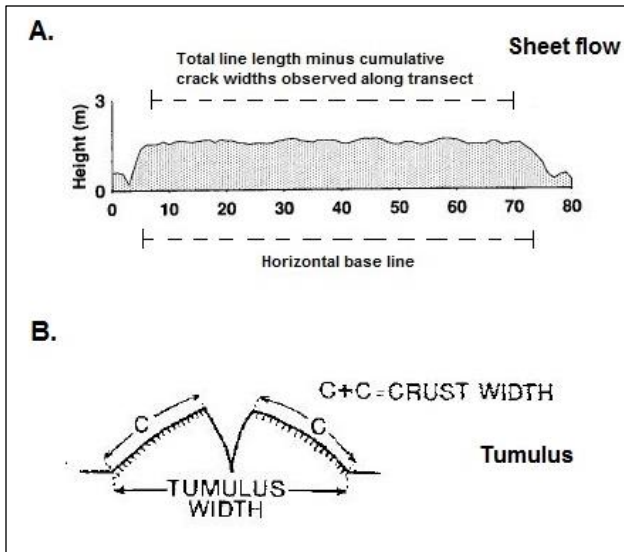


Figure 12 – (A) The cumulative crack widths observed in a transect across the top of a pahoehoe sheet flow should demonstrate at least 1% of extension when compared to a horizontal base line. This indicates brittle fracturing that resulted from inflation. *Adapted from Hon et al. (1994)* (B) According to the criterion for tumuli formation developed by Walker (1991), the total crustal width (indicated by C+C) should be equal to or less than the total width of the structure (the tumulus width) if the cause of the cracking is up-swelling, not lateral pressure. Up-swelling as a cause of cracking would strongly suggest inflation as a mechanism of uplift. *Walker (1991)*

stagnant area, producing inflation pits.

Vertical uplift scarps have also been described by Hoblitt et al. (2012) as a subordinate style of inflation cracking.

Self et al. (1998) recommend

distinguishing between inflation pits and collapse pits by searching for horizontal cracks around the pits that only form

during inflation.

Chapter Three:

McCartys Flow Field Work

The field work on the McCartys Flow at and around the Lava Falls area of El Malpais National Monument had two primary objectives: (1) development of a model to categorize the different kind of crack systems seen on the flow, and (2) measurement of several differential GPS (DGPS) transects on and across the flow and its margins as well as measurements of crack widths and depths within these transects. The crack systems model developed in the field by Dr. Christopher Hamilton divided observed crack systems into three classes based on curvature, fracture style, and spacing (Figure 13). These classes applied mostly to cracks observed at the plateau margins and the depressions in the middle of the plateau. Linear cracks occurring along the plateau margins with no curvature and often located near the top of rotated slabs of crust in a parallel fashion were categorized as Type A. This type of crack encompasses the en-echelon and deep margin cracks observed by Walker (1991) and Hon et al. (1994), as well as the tilted slabs of crust described by Hoblitt et al. (2012). Smaller concentric cracks occurring along convex segments of the plateau margin and around the depressions on the plateau were categorized as Type B. Polygonal crack networks along segments of the flow margins with a positive curvature were classified as Type C. Given its development in the field based primarily on observations, these crack classes proved to be moderately effective at classifying crack systems observed along the plateau margins while in the field. A total of eight DGPS transects were carried out around the Lava Falls area and across the McCartys Flow plateau (Figure 14). DGPS is an enhancement to regular GPS through the establishment of a base station on the ground with a known location.

The base station receiver then calculates its position from satellite signals, comparing this location to its known location. This differential is then applied to the GPS data recorded by the

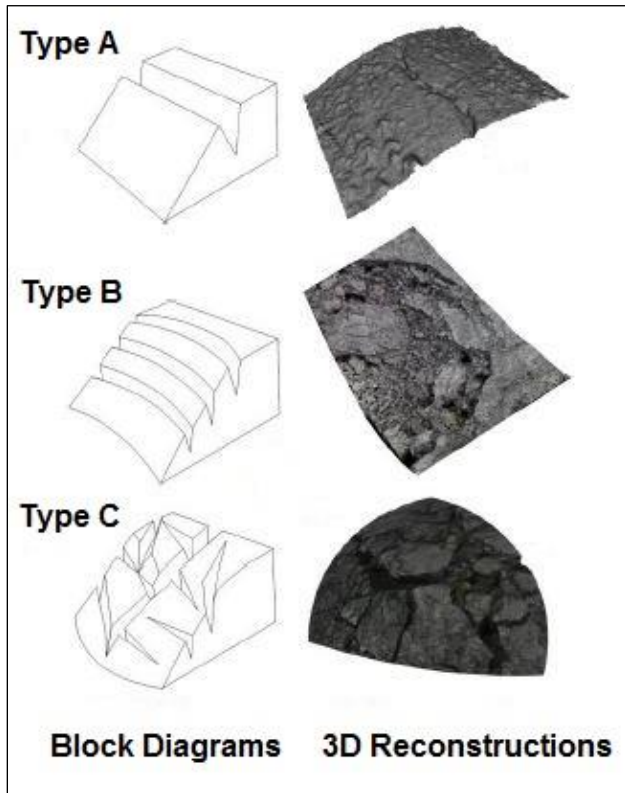


Figure 13 - Block and photogrammetric reconstructions of the three classes of cracks observed on the plateau margins of the McCartys Flow near Lava Falls. Type A – linear, no curvature, hinge-like. Type B – concentric, convex surface. Type C – polygonal networks, concave surface. Adapted from Scheidt et al. (2014)

rover unit. This differential can be applied by two processing methods: Real-Time Kinematic (RTK) and Post-Processing Kinematic. RTK is quicker to calculate because the differential is applied later, but requires a direct line of sight with the base station. PPK requires a processing period to formally calculate the differential, but does not need to be within sight of the base station. Waypoints are recorded using the rover unit and store information such as geographical position (UTM coordinates), elevation, and any notes the surveyors want to manually add. The resulting data can be

later retrieved and displayed in a CSV file in a spreadsheet program like Microsoft Excel.

Transects A, B, C, D, E, and F were mapped using RTK. Transects G and K were mapped using PPK with a 10- second processing interval (Figure 15). The transects were initially laid using duct tape and aluminum foil coated rocks. During surveying, all cracks, margins, local features and textures were noted and in most cases measured and photographed. Transects A-F focused on the Horseshoe area, particularly the monocline on the eastern margin of the plateau.

Transects G and K focused on the profile of the plateau, as well as three major depressions on the flow in the case of Transect K. Accompanying the DGPS data were detailed observations taken at every single stored waypoint, noting the waypoint number, defining features such as the

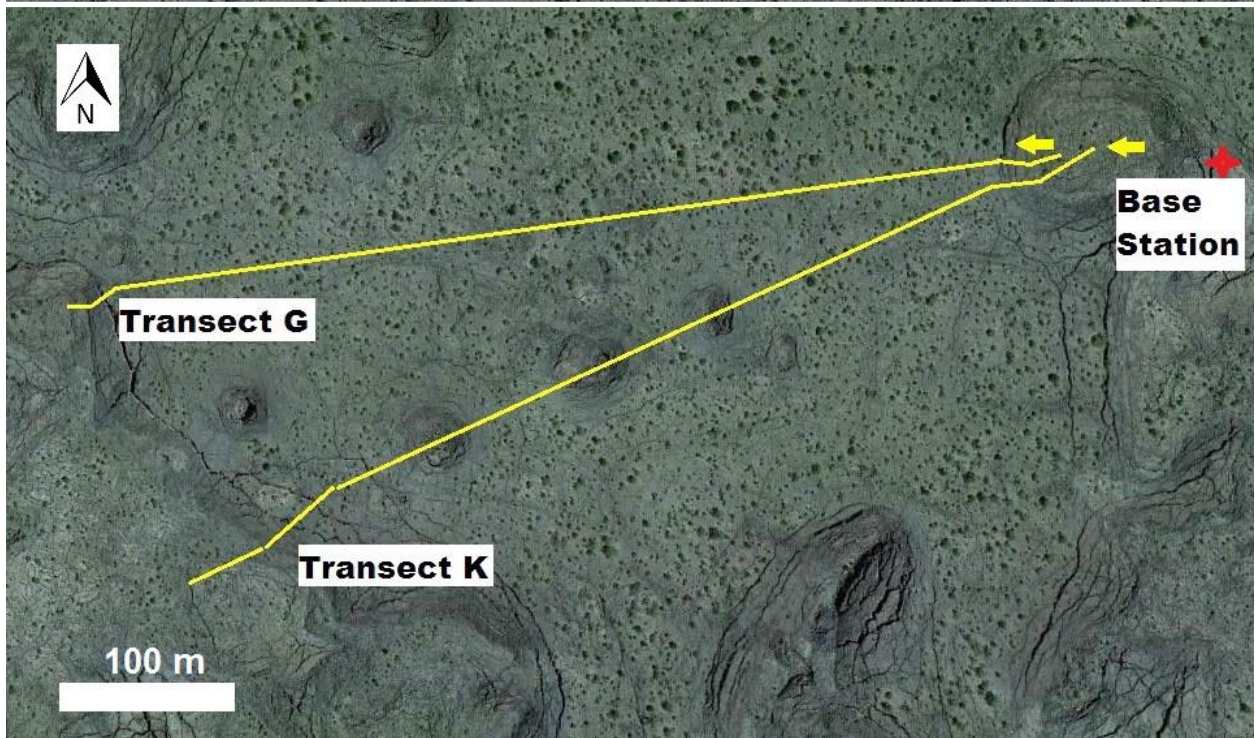
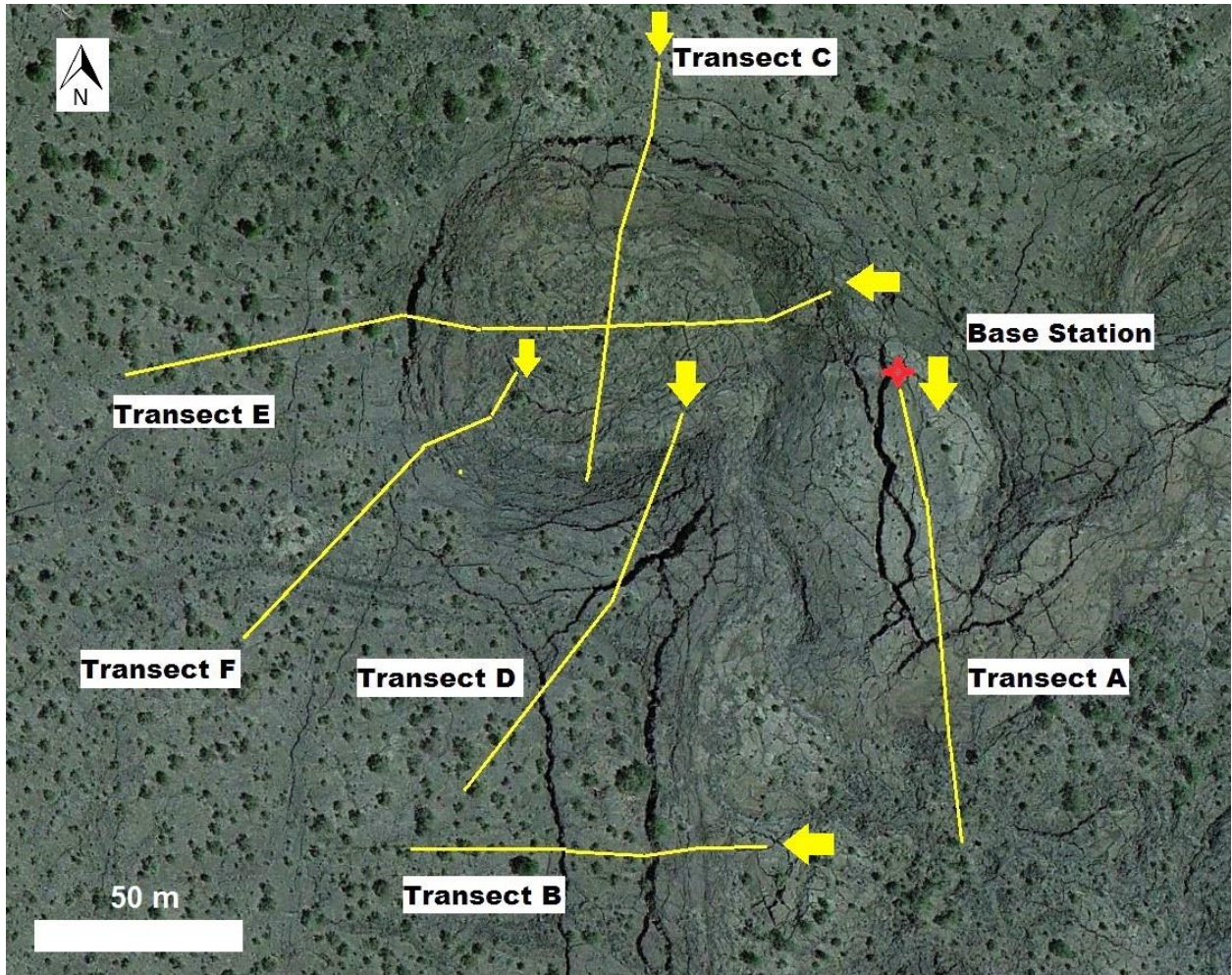


Figure 14 – Locations of the transects mapped around the Horseshoe (top) and across the McCartys Flow plateau (bottom). The yellow arrows indicate the direction of mapping and the red cross is the location of the base station. More precise details about each transect are given in the table in Figure 15. Adapted from Google Earth

Transect ID	Location		Processing	Waypoints	Cracks
	Start	Finish			
Transect A	Top of Horseshoe, east side	Lava Falls area	RTK	26	4
Transect B	Lava Falls area	Top of the plateau, east side	RTK	21	2
Transect C	North of Horseshoe on plateau	Horseshoe basin, south side	RTK	49	5
Transect D	Horseshoe basin, south side	Top of the plateau, east side	RTK	45	3
Transect E	Top of Horseshoe, east side	Top of plateau, east side, west of Horseshoe	RTK	70	7
Transect F	Horseshoe basin, west side	Top of plateau, east side	RTK	40	7
Transect G	Horseshoe basin, west side	Base of the western monocline, opposite side of the plateau	PPK, 10-second interval	163	23
Transect K	Horseshoe basin, center	Base of the western monocline, opposite side of the plateau	PPK, 10-second interval	268	40

Figure 15 - Table summarizing the DGPS transects taken on and across the McCartys Flow at the Lava Falls area. Transects are identified by their ID. Descriptions of the starting and finishing points, the processing method, number of waypoints, and number of cracks measured is given for each transect. The locations of each transect are displayed on the map in Figure 14.

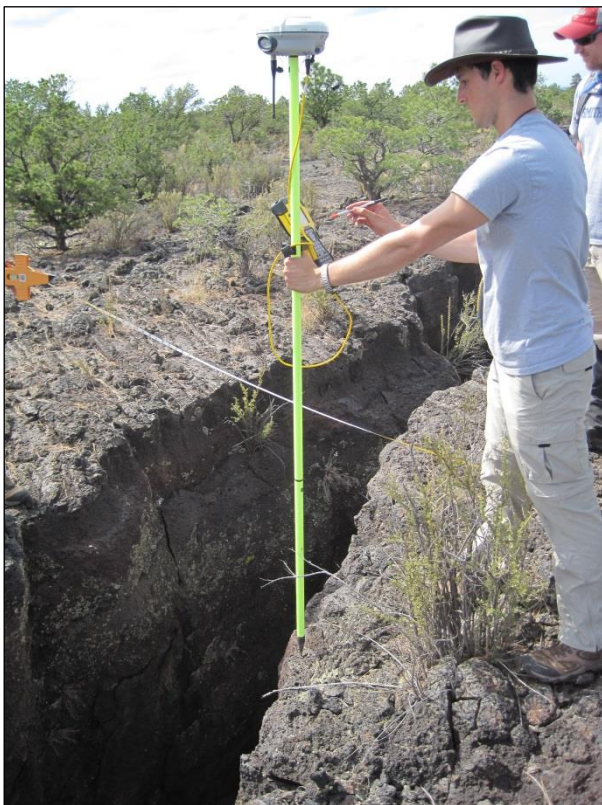


Figure 16 - Ryan Samuels using the DGPS rover unit and tape measure to measure across a crack up on the plateau.
Charles Wise

texture of the flow, presence of a crack, points of inflexion, presence or absence of slope, contacts, and crack widths and depths taken at every crack traversed using a measuring tape weighted with a rock. For the sake of accuracy, handheld GPS units were also used to record waypoints of cracks and other defining features such as contacts and changes in slope.

Chapter Four:

Analysis of the Crack Classification Model and DGPS Data Sets

The crack classification was tested by loading base maps of the Lava Falls area of the McCartys Flow obtained from Google Earth into the program ArcMap and using the line tool to map out the cracks visible on the flow and the approximate flow and plateau margins. These maps of crack patterns were analyzed for their usefulness at distinguishing crack patterns in a remote sensing environment.

Type A cracks were almost exclusively observed at plateau margins as singular, large, hinge-like cracks (Figure 17). Several parallel subordinate cracks are also observed at the base of the plateau monoclines, consistent with the tilted-slab cracking observed by Hoblitt et al. (2012) (Figure 17). These cracks were among the deepest and widest observed on the flow, ranging as much as 7-8 m in depth and 1-2 m wide. Some examples of these cracks were tens of meters long, extending along the margin in a relatively uninterrupted fashion as long as the margin remained linear. Several examples of these cracks also had rubble that had accumulated inside the fracture, complicating the measurement of depths. Hoblitt et al. (2012) model the tilted-slab cracking as propagating down to the viscoelastic layer during formation, suggesting that the deepest part of the fracture would represent the boundary between the pre-existing viscoelastic layer and the substantially thickened brittle crust. Hon et al. (1994) developed the equation $t = 164.8C^2$ to calculate the amount of time elapsed since crustal growth began on an active flow (t – hours) based on C (depth of a crack system in meters). With a maximum crack depth of 8 m, a minimum of 1.2 years is estimated for the duration of active uplift on this part of the McCartys Flow, suggesting that the supply of lava from the McCartys source to the south was active for a least this period of time and accounts for the substantial depths of some of the

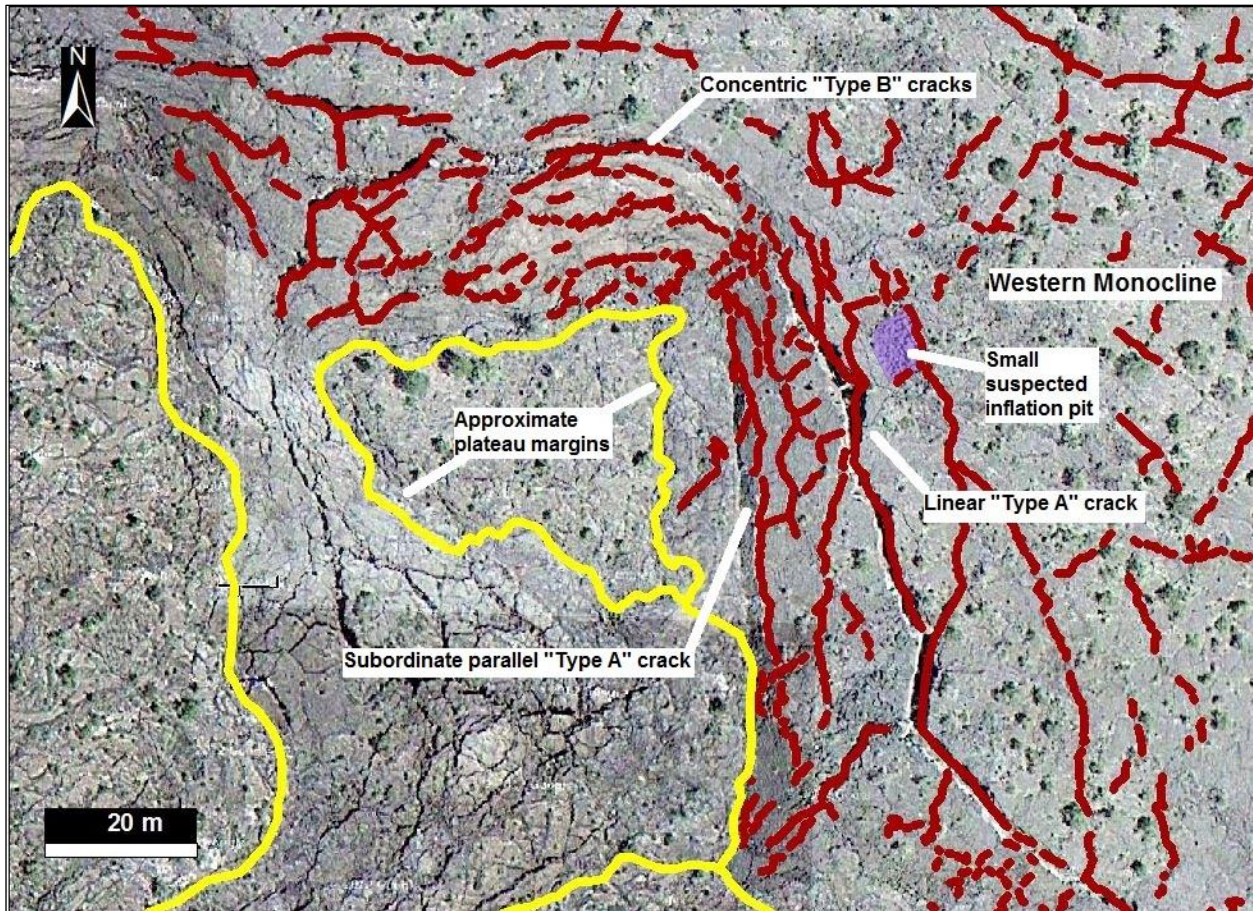


Figure 17 - ArcMap crack systems map from the western edge of the McCartys Flow on the plateau margin. Red lines are cracks, yellow lines are the approximate plateau margins, and purple are depressions. Note the dominant linear Type A crack to the left of center on the flow margin and the parallel subordinate linear crack running along the base of what appears to be a large tilted slab. Concentric Type B cracks are also present on the northern part of the margin.

cracks observed near the Lava Falls area. Type A cracks were easily recognizable in the crack systems maps developed using remote sensing images of the McCartys Flow as a single, linear line on the plateau margins (Figure 17), implying no curvature of the flow surface at that point. Field observations and images of the western monocline of the plateau mostly confirm this lack of curvature (Figure 18), suggesting that the Type A crack classification is effective at describing both the nature of the crack system as well as the absence of curvature on a margin in a remote sensing image of a pahoehoe sheet flow.

Type B cracks were observed both at flow margins (Figure 17) and predominantly around the depressions on the southern part of the McCartys Flow (Figure 19), consistent with the

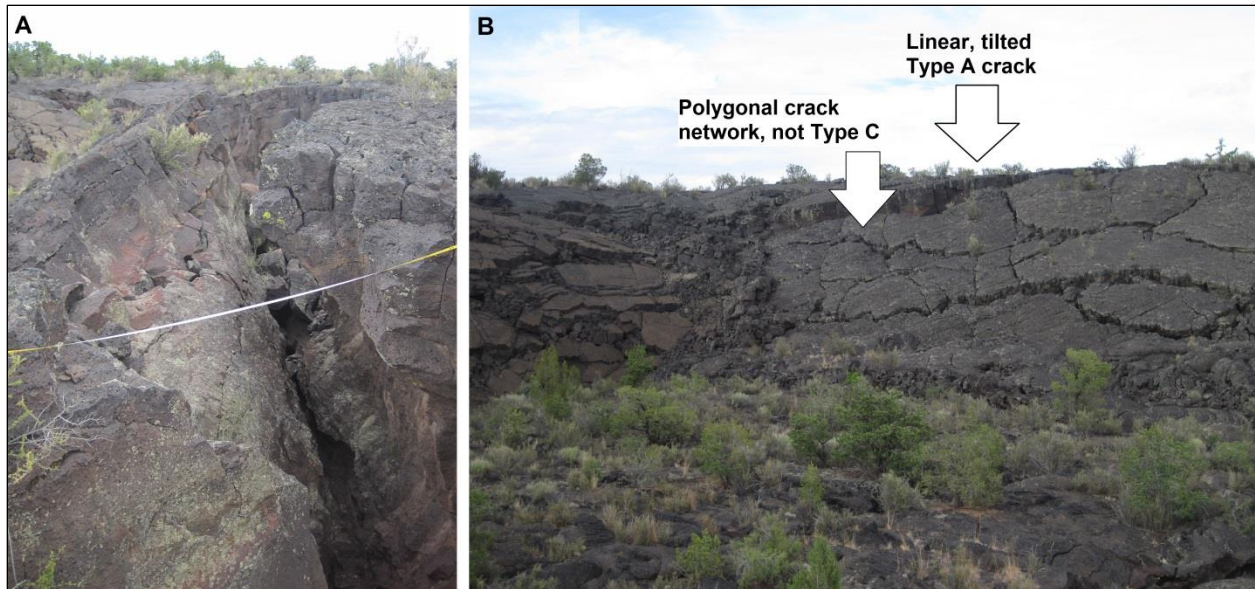


Figure 18 – (A) The large linear Type A crack indicated in the ArcMap crack systems map in Figure 17. Note the substantial width of the crack as the lower block appears to be tilted and the presence of rubble in the fracture. (B) The location of the large linear Type A crack on the western monocline of the plateau. Note the lack of any significant curvature along the margin where the crack exists, although the crack networks on the tilted block resemble a polygonal Type C crack system. *Charles Wise*

expectations of the model. These cracks ranged in depth from 1-4 m at the three depressions and 0.5-2 m on the plateau margin at the Horseshoe. This disparity is explainable due to the presence of down-dropped and tilted blocks at the depressions that seem to indicate a similar kind of movement compared to the rotated slabs of the linear Type A cracks, but are not able to be classified as such because of their concentric shape. The smaller crack depth range for Type B cracks observed on the plateau margins is explainable by the lack of observed tilted slabs on the margin compared to the depressions. Small, thin concentric cracks were also observed at a regular distance from the three main depressions. Had the depressions formed from the collapse of a roofed-over lava tube, overbank lava consisting of crustal blocks ranging from 5-10 cm wide and 3-5 cm thick displaying a smoother, lineated texture on one side and a rough, jagged texture on the other would be present. Overbank lava is observed on the Bandera Flow to the northwest of the McCartys near several significant well-defined lava channels that flow away from the

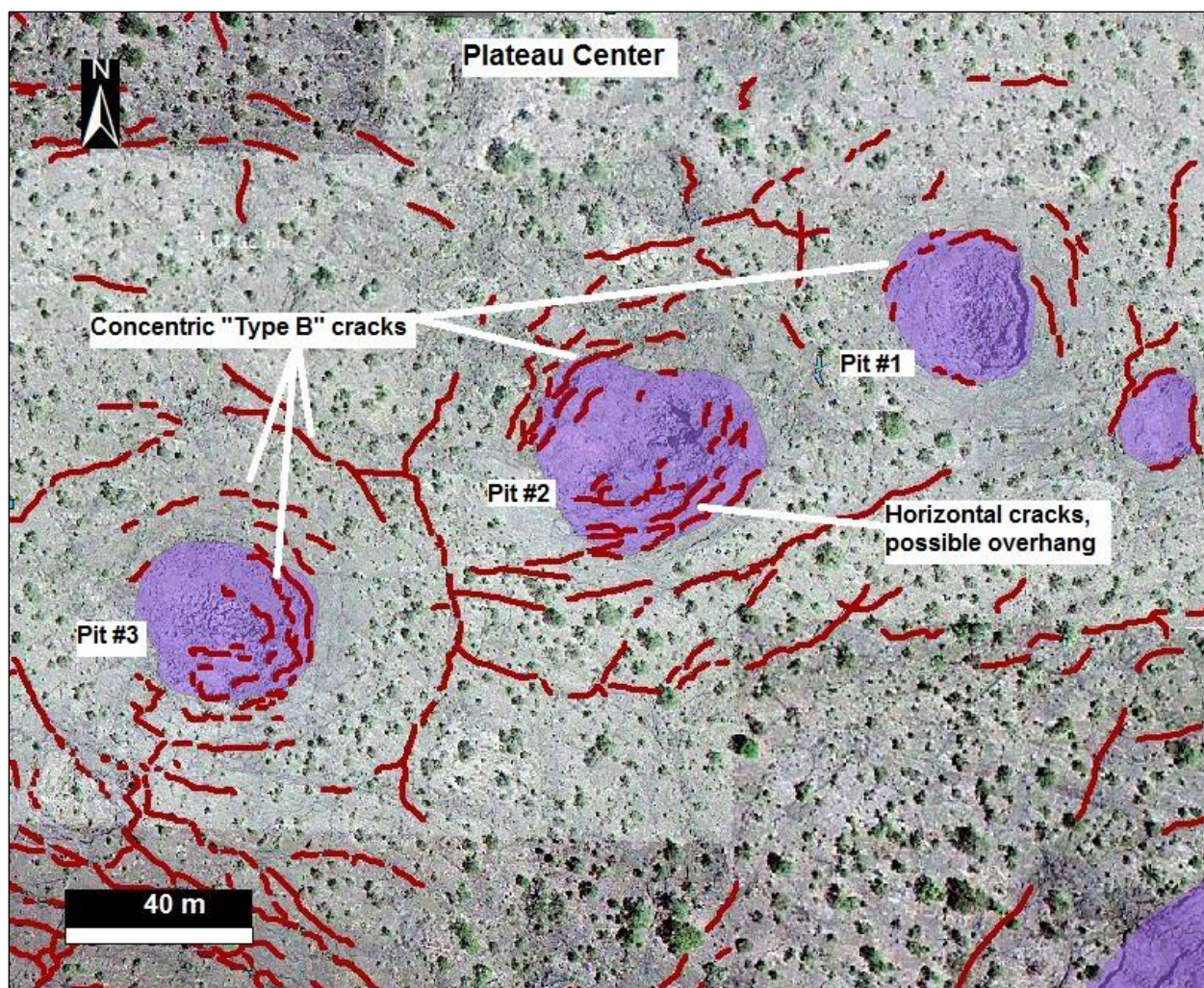


Figure 19 – ArcMap crack map of the three depressions located on the plateau on the southern part of the McCartys Flow. Note the concentric cracks in Pits #3, #2 and #1, as well as the presence of smaller concentric cracks spaced outwards from the depressions. There is also a possible overhang in Pit #2 along with some more linear cracks.

Bandera Crater. Furthermore, the concentric crack spacing is more indicative of bifurcation of the flow around an object as opposed to the channelization of the lava in a lava tube through all three depressions. In this regard, the remote sensing crack maps of the depressions do a reasonable job at disqualifying a collapsed lava tube hypothesis but are still best confirmed through our field observations on the ground. Images of Pits #3, #2, and #1 (Figure 20) show concentric cracking on concave surfaces, significant tilting of cracked slabs, and relatively smooth lava textures around the outsides of the depressions that are not indicative of overbank lava that would normally be observed near a lava channel.

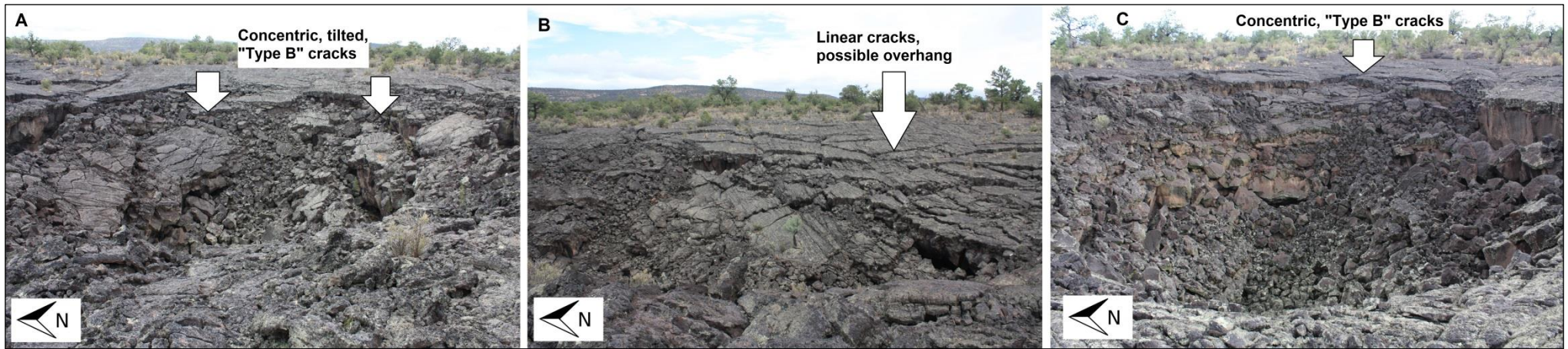


Figure 20 - (A) Pit #3 on the McCartys Flow displaying concentric, tilted, Type B cracks. (B) Pit #2 showing the sub-linear to linear cracks near a possible overhang. (C) Pit #1 displaying typical concentric Type B cracking and a significant accumulation of rubble in the pit. All pits have relatively smooth, billowy surfaces around the outside, which contrasts to the slabby, jagged overbank lava that would be present if the pits were a collapsed lava tube or roofed-over lava channel. *Chris Hamilton*

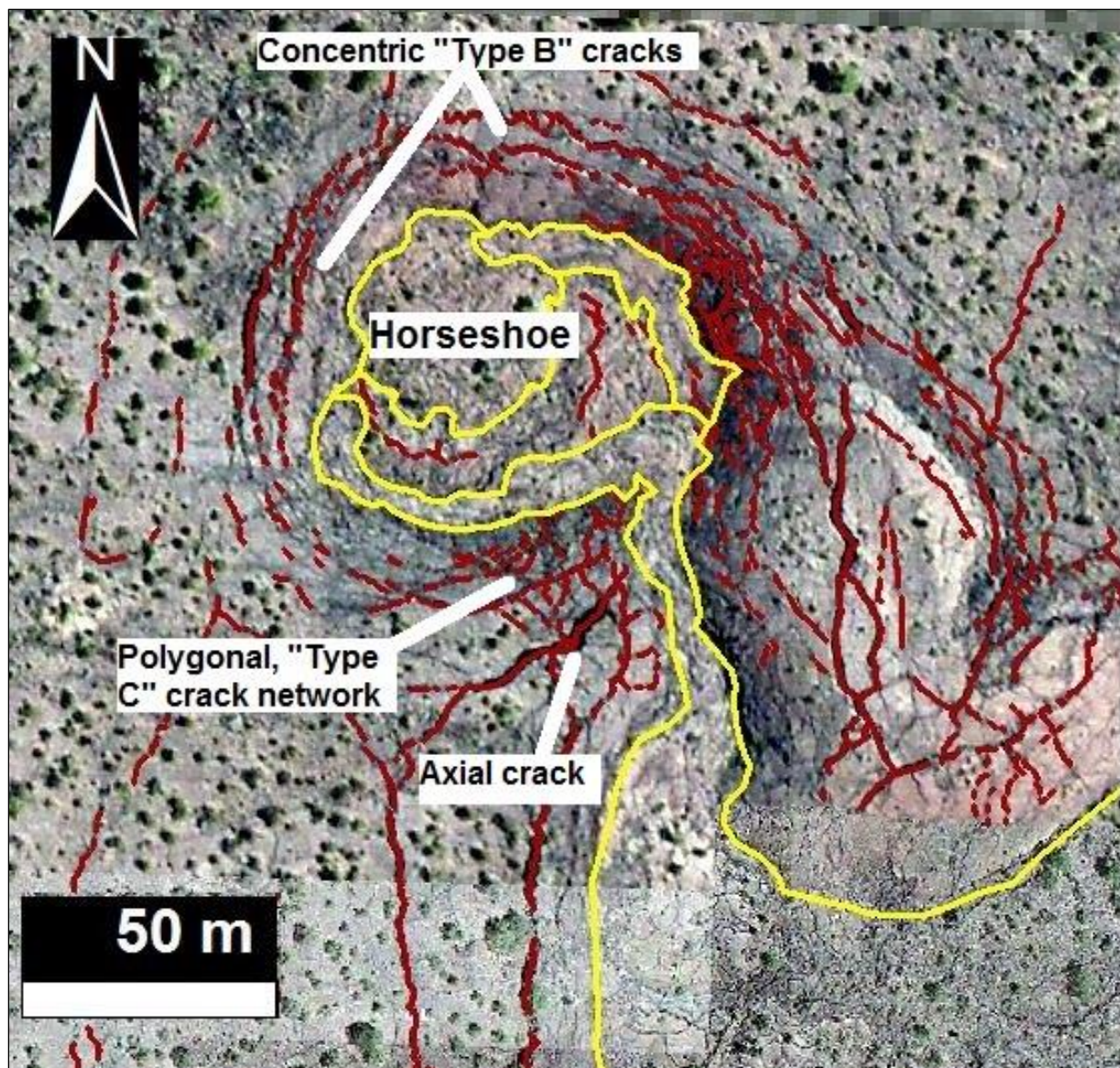


Figure 21 – ArcMap crack systems and approximate flow and plateau margins map around the Horseshoe area of Lava Falls. Concentric Type B cracks are visible along the eastern and northern slopes. The best example of the polygonal, Type C crack network is visible on the southern slope of the Horseshoe. See Figure 22 for an image of the crack network.

Type C cracks were only observed on the plateau margins near and around the Horseshoe on the eastern monocline of the plateau. They consisted of a series of polygonal cracks often surrounding a deeper, axial crack that cut through perpendicular to the network. The particular example of Type C cracking observed on the southern slope of the Horseshoe did display a positive curvature; however, the ability of mapped Type C cracks in remote sensing

environments to describe the curvature was much more limited and not very accurate. For example, possible Type C cracking was also observed on the western monocline further down the slope from the dominant linear Type A crack (Figure 18), which suggests that this polygonal crack network is occurring on a tilted slab instead of on a surface with a positive curvature, as indicated by the presence of the subordinate, linear crack parallel to the dominant crack at the base of the slope. It might be suggested that Type C crack networks be further qualified in remote sensing environments by examining their location relative to other crack types (such as Type A cracks in the aforementioned case) or looking for examples displaying an axial crack cutting through the network, as is the case in the example found in the Horseshoe (Figure 21). Without these features available for confirmation, it would be difficult to reliably apply the Type C crack pattern in a remote sensing environment.



Figure 22 – Looking southwest at the southern slope of the Horseshoe at the polygonal Type C crack pattern visible on a positive curvature. Note the significant axial crack cutting through the polygonal network. *Andrew de Wet*

Analysis of the DGPS transects was carried out in Microsoft Excel to generate elevation profiles and crack dimensions analysis. Crack positions were calculated in by subtracting the crack depths from the elevations of the crack margins to produce a rough indicator of their position. This method is mostly useful visually to understand the distribution of cracks within the transects, because it does not account for the internal behavior of the cracks such as the orientation of their propagation and their changes in width and depth. The resulting profiles with cracks included can be found in the Appendix.

Transects G and K, taken across the entire plateau and through the three depressions on the southern part of the flow, respectively, demonstrated several good indicators of inflation as the mechanism of uplift for the plateau and also suggested a possible inflation history for the area. Firstly, the elevation profile of Transect G (Figure 23) confirms that the plateau is a smooth inflated pahoehoe sheet flow bounded at both sides by monoclines, consistent with an emplacement history of laterally coalescing lobes on a relatively flat ($1-2^\circ$) slope. The bowed nature of the plateau in the middle with a relief of 2-4 m is probably a result of deflation of the plateau after the supply of lava to the area diminished in the later stages of eruption. Analysis of the plateau structure by the methods of Hon et al. (1994) and Walker (1991) was carried out using two sets of data: 1) the absolute width of the plateau determined from two specific UTM coordinates, and 2) measures of absolute crustal width across the transect. The first metric calculates the width of the plateau as a horizontal base line, and the second metric utilizes the ability of Google Earth to display digital elevation maps to calculate the crustal width more accurately. By qualitatively determining through field observations of each DGPS waypoint where the slope of each monocline at the edge of the plateau began, the overall structural width

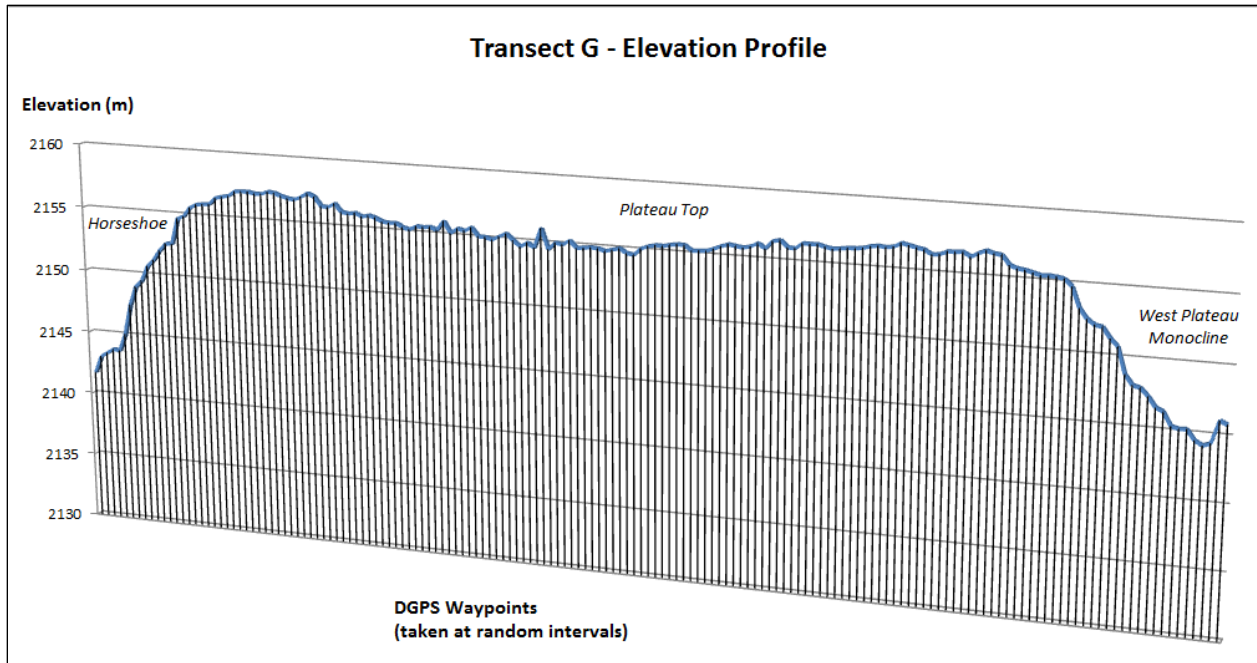


Figure 23 - The elevation profile of Transect G (without the cracks added), generated from the DGPS data collected. The flow surface varies only a little in regards to elevation and suggests a smooth inflated pahoehoe sheet flow. The minor relief in the center of the plateau is interpreted as deflation after the supply of lava to the area began to dwindle.

was measured by determining the distance between known UTM coordinates at both points by the Pythagorean Theorem:

$$\text{Northing } 1 = N_1, \text{ Easting } 1 = E_1, \text{ Northing } 2 = N_2, \text{ Easting } 2 = E_2$$

$$\sqrt{((N_1 - N_2)^2 + (E_1 - E_2)^2)} = \text{Distance in meters}$$

The absolute crustal width was obtained by using the same UTM coordinates and the Path tool in Google Earth to measure the distance along the topography between each coordinate. The cumulative crack widths within these two waypoints were calculated from the DGPS data set and subtracted from the absolute crustal width to obtain the total crustal width, accounting for the separation of the crust by the cracks. This value was compared to the measured structural width and a percent difference was obtained (Summarized for all transects in the table in Figure 24). For Transect G, the absolute width was approximately 548 m, compared to a crustal width of approximately 540 m, producing a percent difference of about 1.6%. This falls comfortably

Transect ID	Structural Width (m)	Absolute Crustal Width (m)	Cumulative Crack Width (m)	Crustal Width (m)	% Difference
Transect A	82.47	82.40	2.74	79.66	-3.41
Transect B	85.10	85.80	4.05	81.75	-3.93
Transect C	62.03	61.60	5.90	55.70	-10.20
Transect F	115.24	115.00	4.85	110.15	-4.41
Transect G	548.08	548.00	8.48	539.52	-1.56
Transect G - West End	22.67	23.00	4.50	18.50	-18.40
Transect K - East End	115.39	116.00	3.69	112.31	-2.67
Transect K - West End	47.72	47.00	6.32	40.68	-14.75

Figure 24 - Table of percent extension across measured transects comparing the structural width of the transect (measured using UTM coordinates and the Pythagorean Theorem), the absolute crustal width (calculated in Google Earth using the Path tool between the two UTM coordinates), and the cumulative crack width (the sum of all crack widths measured on the transect in between the UTM coordinates). The percent difference between the newly calculated actual crustal width and the structural width should range from 1-2% for features where cracking was caused by up-swelling of lava, in essence inflation. The total extension of Transect K was not measured because it contained the three depressions and Transect E was omitted because it crossed the Horseshoe and featured cracks not part of the plateau. The high percentages of extension in Transects C, G (West End) and K (West End) are assumed to be the result of being unable to measure the true absolute crustal width due to the plateau margins being obscured by breakouts.

within 1%-2% range of extension expected for sheet flows where the cracking on the flow was caused by up-swelling (Hon et al. 1994; Walker 1991). Smaller scale analysis of the end members of the two largest transects (Transects G and K) were also carried out to analyze the amount of extension present on the plateau margins. The percent difference for all end members with the exception of Transect K (East End) were abnormally high compared to the expected 1%-2% hypothesized by Hon et al. (1994). There are several factors that might account for this disparity. Firstly, the margins of the plateau are often obscured by debris, rubble, breakouts, toes, and smaller lobes and flows that make it difficult to ascertain the true absolute crustal width of the member. This is evident in the elevation profile of Transect K that includes the three depressions. The elevation of the bottom of Pits #2 and #3 in the elevation profile are shown to be lower than the elevations of the base of both plateau margins; Pit #2 by as much as 2-3 m compared to the elevation of the Horseshoe basin and 3-6 m compared to the eastern monocline base, and Pit #3 by as much as 4-5 m compared to the Horseshoe basin and as much as 6-7 m compared to the eastern monocline base. Hon et al. (1998) suggests that the depths of these depressions on inflated flows correspond approximately to flow thickness. Therefore, the actual

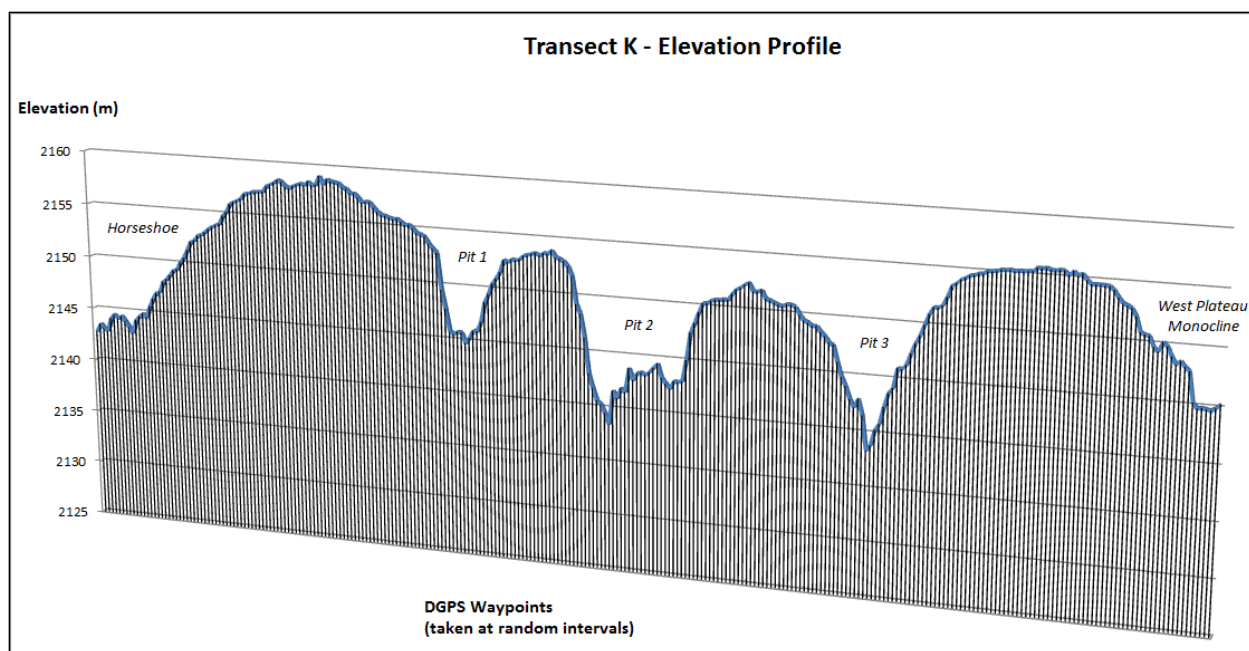


Figure 25 - Elevation profile of Transect K including the three depressions on the southern part of the flow. Note that the elevations at the bottom of Pits 2 and 3 are lower than the elevations of the bases of the monoclines, explaining the large percentage difference between the absolute widths and crustal widths of the end members of Transects G and K.

depth of the flow as approximated by the deepest depression (Pit #3) measured to a local high point in Transect K (near the western plateau monocline) would be roughly 15-17 m. This suggests that the obscured plateau margins may extend as much as 5-8 m further below the surface. Secondly, our calculations for the end members of the transects did not account for the curve of the slope, since our data set was not complete enough to apply a modified calculation to account for this. Finally, this particular method of analyzing extension on slope is a departure from the methods employed by Walker (1991) in calculating extension in tumuli and Hon et al. (1994) who looked at extension across the top of smooth pahoehoe sheet flows and not on the slopes of the margins. This data is therefore not particularly useful at saying anything in regards to extension because the proper measurement of the absolute crustal width could not be obtained and the curved nature of the line segment representing the flow margins requires a more refined mathematical approach, such as the development of a curve of best fit using a modified Euler's method or a similar means of approximation.

Hon et al. (1994) also graphed crack widths versus crack depth across a smooth pahoehoe sheet flow profile to suggest by means of a linear trend between the two crack dimensions that inflation of the flow was relatively constant. A graph of these data points for Transect G (Figure 26) showed a weakly linear trend between the crack widths and crack depths on the transect, suggesting that inflation of the McCartys Flow near Lava Falls might not have proceeded in a constant manner. The graph in Figure 26 shows that crack widths increase at a more substantial rate than corresponding crack depths, suggesting that inflation on the flow was responsible for adding a substantial amount of new upper crust to the flow that would have continued to crack and expand with uplift but because of the thickness involved compared to the types of recent flows examined by Hon et al. (1994), the cracks may not have been able to propagate as deeply

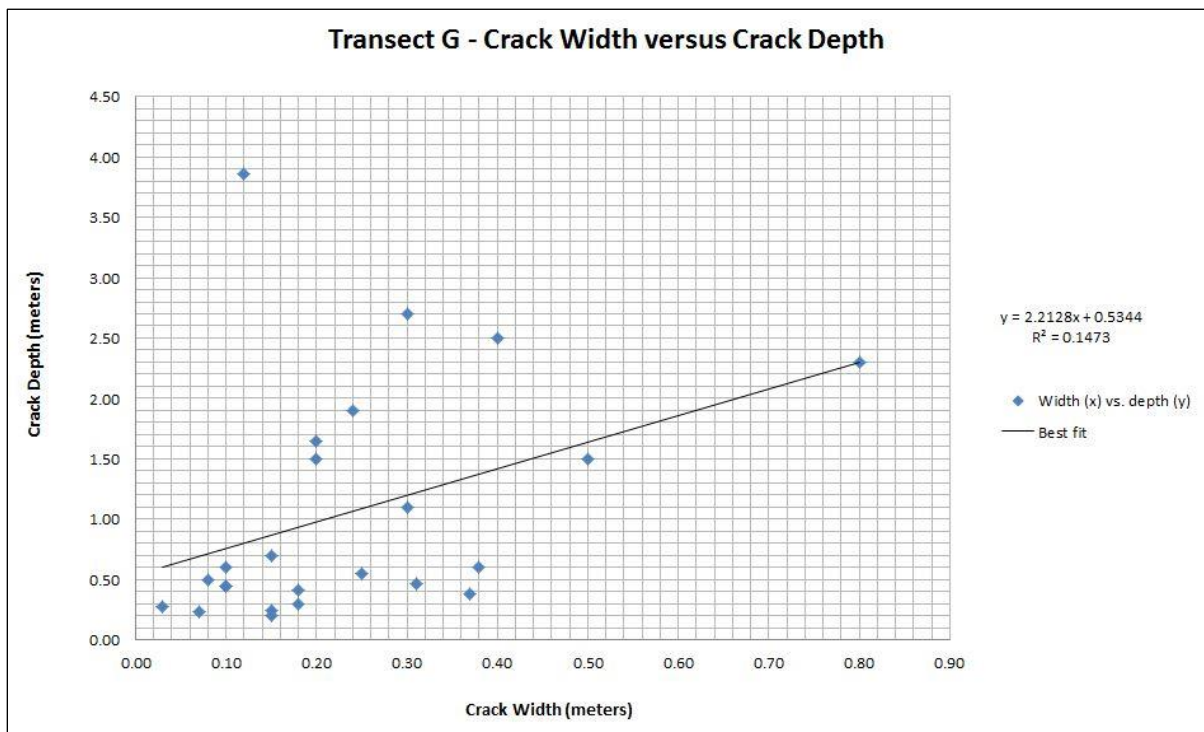


Figure 26 – A graph of crack widths versus crack depths along Transect G across the plateau. Two substantially deeper cracks found close to the flow margins were removed from the data set because they were more closely related to tilting of slabs on the margins than to the kind of extension Hon et al. (1994) were seeking to measure. The crack with the unusual depth of almost 4 meters (circled) was found in the middle of the flow and could possibly be part of a small tumulus, though field notes collected at this waypoint during surveying do not indicate a local topographic high. The linear trend extrapolated here suggests that crack width expansion occurred at a greater frequency than crack depth propagation during uplift.

because the accumulated crust would be relatively thick and less brittle. The deepest cracks measured in the transects are almost exclusively found at or near the plateau margins or near the depressions in the middle of the flow, where slab tilting and scarp formation ensure deeper crack formation.

Another explanation of the lack of a clear linear trend between crack depth and crack width may be a circumstance of the emplacement history of the McCartys Flow. The elevation profile of the southern McCartys Flow from the vent down to the Lava Falls area (Figure 27) shows a series of plateaus of decreasing elevation, with the various depressions on the flow occurring as local topographic lows. Based on this topographic model, a model of emplacement

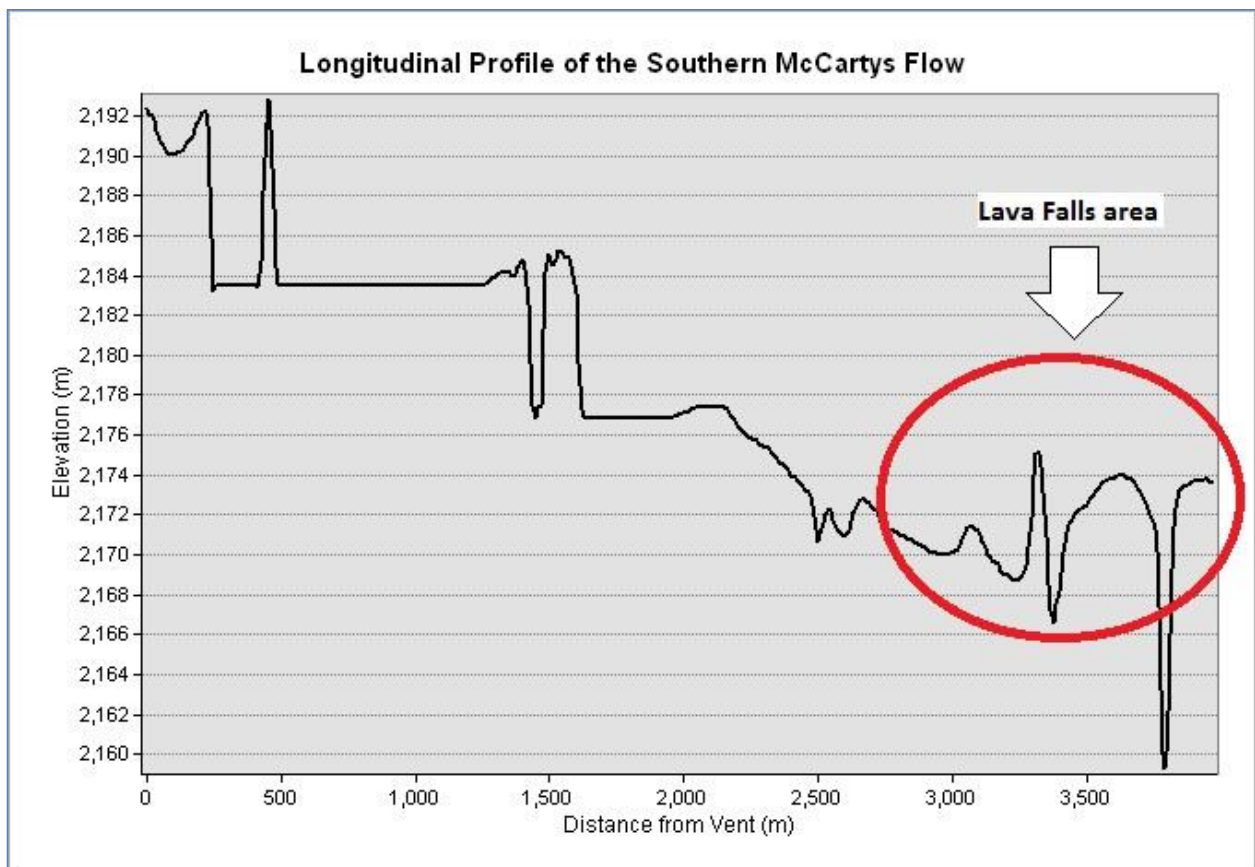


Figure 27 - Longitudinal elevation profile of the southern McCartys Flow from the vent down to the Lava Falls area, generated in ArcMap using 3D-Analyst tools. The successive plateau levels point to an emplacement model (Figure 28) that would also account for the lack of a clear linear trend between crack widths and crack depths across the plateau near Lava Falls.

for the southern McCartys Flow that explains the presence of the various plateaus of decreasing elevation and possibly accounts for the lack of linear trend between the crack widths and crack depths across the plateau near Lava Falls was developed (Figure 28). The model suggests the development of a series of inflated plateaus propagating southward from the McCartys vent. The emplacement of one plateau would have proceeded in a logical fashion with pahoehoe toes coalescing to form lobes, which would then coalesce laterally to produce smooth sheet flows and

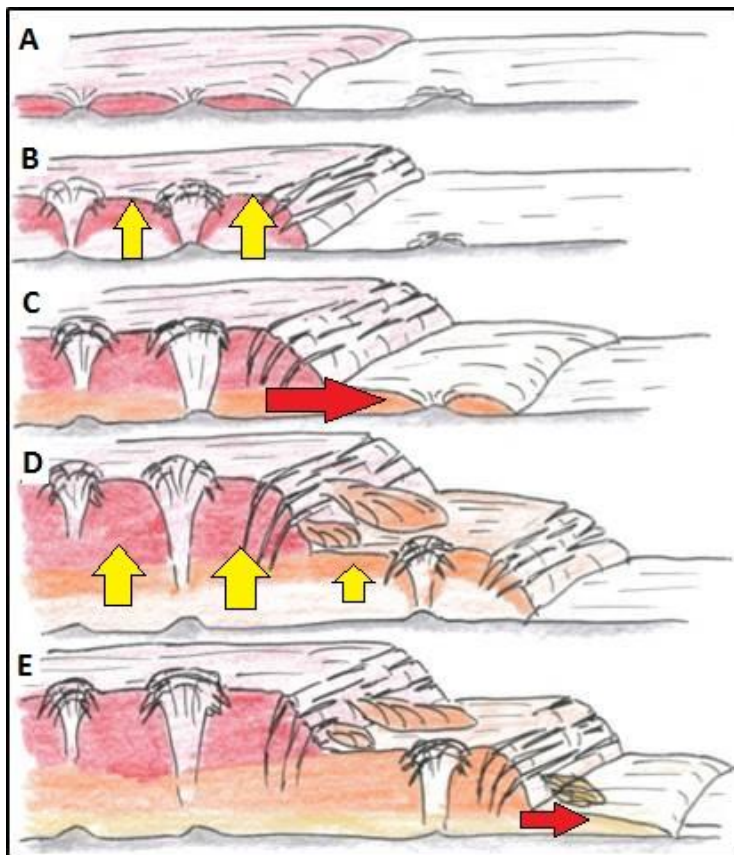


Figure 28 – A sketch of the proposed model of emplacement to explain the lack of a strong linear trend between crack widths and crack depths seen along the plateau of the McCartys Flow near Lava Falls. (A) Initial emplacement of the first smooth pahoehoe sheet flow. (B) Inflation of the first sheet flow to form a lava-rise plateau. Previous topographic highs form inflation pits. (C) A breakout occurs and inflation of the plateau ceases while lava is fed to the new area via developed insulated pathways. (D) Once emplaced, the second flow begins to inflate and the first plateau undergoes renewed inflation due to the presence of uniform hydrostatic pressure across both areas. (E) A second breakout occurs and the emplacement of a possible third plateau begins. *Andrew de Wet*

eventually producing a hydrostatically-linked flow field that could uniformly inflate. Eventually, a new breakout could occur at the edge of the plateau and the lava from the vent could continue to feed the breakout through the developed pathways in the old plateau and begin the process again, assuming that the supply of lava continued at a reasonable rate. Because the older plateau would initially stop inflating after the occurrence of the breakout, a significantly smaller amount of new crust would be generated during this time and so crack depths would stop propagating any deeper into the

flow because they would reach the viscoelastic layer after only a few meters or more. Crack widths would still be able to increase as the crust would probably deflate slightly and tilt. Eventually, after the second plateau had been emplaced and began to inflate, both plateaus would experience uniform hydrostatic pressure, allowing the first plateau to start inflating again while the second plateau began initial inflation.

The lack of linear trend on the plateau near the McCartys might explain this model because crack widths would increase during the brief period of deflation while crack depths would not. Furthermore, the elevation profile of Transect G across the plateau shows evidence of mild deflation of up to 3-4 m (Figure 23), which could be the result of inflation being briefly halted as a new plateau was emplaced.

Chapter Five: Applications to Mars

Considering the moderate effectiveness of the crack systems classification for linear Type A cracks and concentric Type B cracks in both the field environment of the McCarty's Flow and in subsequent mapping of the crack systems using remote sensing images in ArcMap, the possibility of applying parts of the classification model to other remote sensing cases, such as in extraterrestrial environments like Mars, is considered the basis of an effective planetary analog study. The Elysium Volcanic Province is the second largest volcanic province on Mars and features three main types of volcanic activity: 1) effusion of lava from point sources or vents, 2) effusion of lava from linear sources and fissures, and 3) caldera formation likely associated with lava effusion (Platz and Michael, 2011). Of these, lava effusion from fissures is of particular interest, especially within the Elysium Planitia, located to the east of Elysium Mons. Hamilton

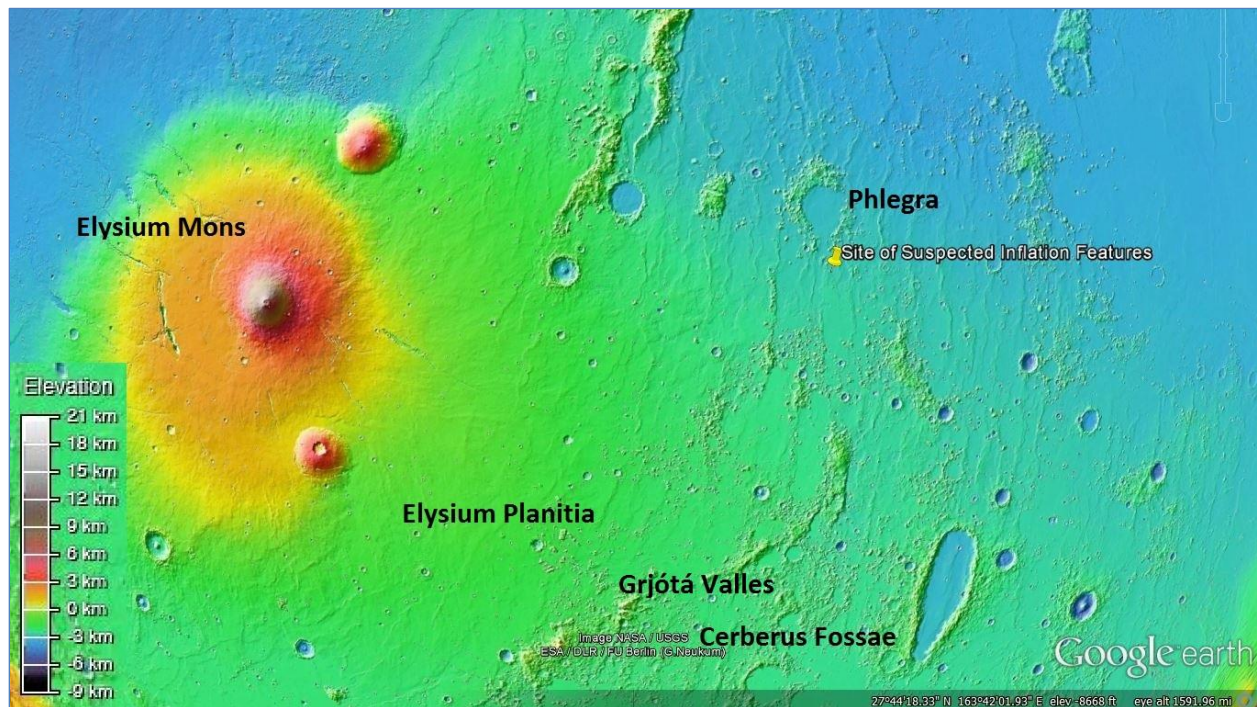


Figure 29 – Colorized terrain map of the Elysium Volcanic Province of Mars with major geographical features labeled. The particular site of interest for analog work is indicated by the yellow pin and is located just south of the Phlegra region. A larger more detailed view of this area is visible in Figure 30. Adapted from Google Earth

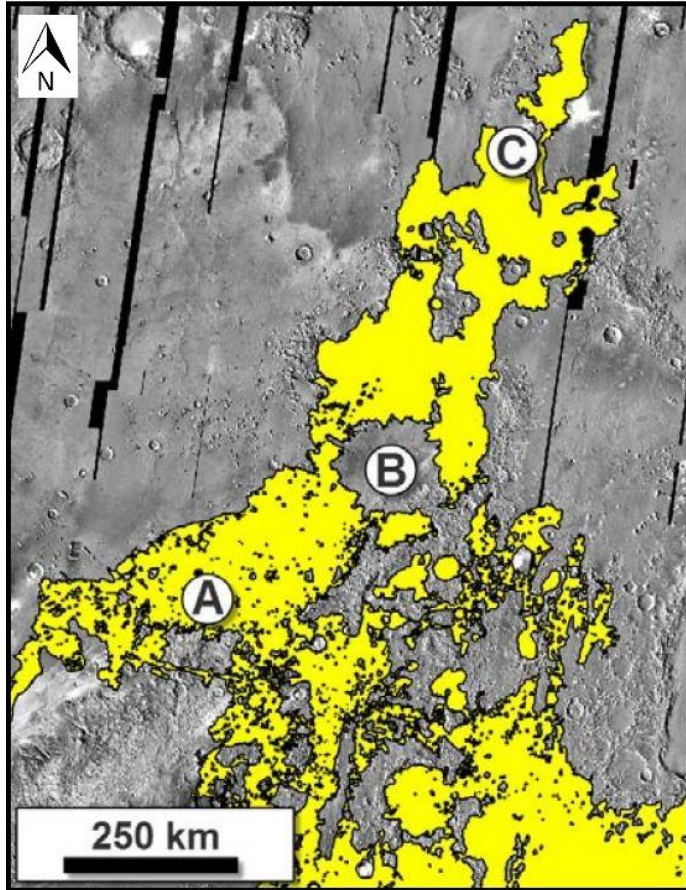


Figure 31 – The northern part of the Cerberus Fossae 2 unit (yellow) extending from its source region in Grjótá Valles (A) past a large unnamed impact crater (B) up as far as Phlegra (C), which contains several suspected inflated lava flow features, visible in the HiRISE image in Figure 30. Adapted from Hamilton (2013)

(2013) has re-examined the Cerberus Fossae 2 unit, which includes regionally extensive flows that appear to originate from the Cerberus Fossae fracture system (Figure 31). According to Hamilton (2013), not only does the Cerberus Fossae 2 unit appear to continue further northwest than previous studies have inferred, but high-resolution Mars Reconnaissance Orbiter (MRO) imagery reveals surface features

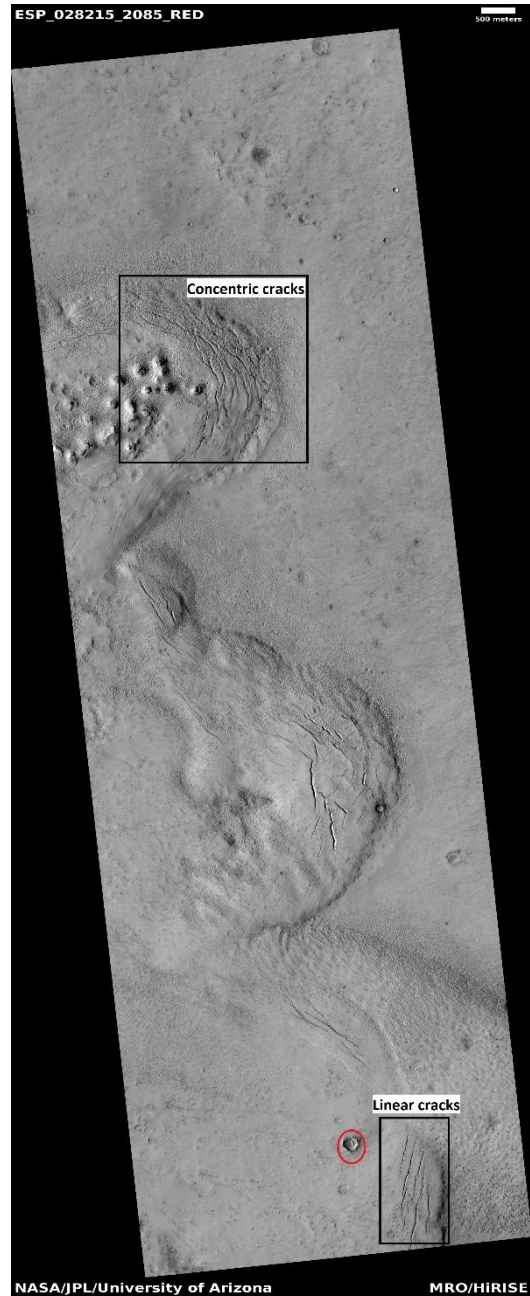


Figure 30 – A HiRISE image of a suspected inflated lava flow located near the Phlegra area of the Elysium region. Note the presence of significant concentric cracks on the margins, as well as several linear cracks. Although no localized cracks are apparent around the depression in the bottom of the image (circled in red), other depressions in neighboring regions on the same flow could exhibit concentric cracking patterns indicative of formation by inflation. University of Arizona HiRISE

demonstrating flow characteristics analogous to inflated pahoehoe flows, such as concentric and linear monoclinical cracks and depressions. Selecting certain High Resolution Imaging Science Experiment (HiRISE) images from the MRO that show analogous inflation features (e.g. Figure 30) would allow for the mapping of the visible crack systems in ArcMap using the classification model developed from the McCartys Flow. Local topographic information such as surface curvature, possible original topography based on the idea of inflated regions as inversions of topography (Self et al. 1998), and the presence of monoclinical slopes indicating either inflation plateaus or flow margins could be extrapolated from the crack systems classification model. Furthermore, the presence of concentric cracks surrounding depressions might be useful in determining whether the depressions were formed as an impact crater or whether they are actually inflation pits.

Chapter Six:

Conclusions

The crack classification model developed for usage in the field proved to be moderately effective at distinguishing crack systems characteristic of the inflation process when mapped and viewed in remote sensing images in ArcMap. Crack types A (linear) and B (concentric) were found on flow margins (Type A and B) and around depressions (Type B), consistent with previous observations regarding crack systems on inflated flows made by Walker (1991), Hon et al. (1994), Self et al. (1998), and Hoblitt et al. (2012). Linear Type A cracks in particular usually demonstrated slab tilting, as discussed in Hoblitt et al. (2012) and were almost exclusively found on or near the plateau margins. Polygonal Type C crack networks were useful as a descriptive tool for categorizing cracks within the Horseshoe area, but proved to be less useful as a diagnostic of the curvature of the terrain in remote sensing images, particularly on the western monocline of the plateau. Overall, the crack classification model proved most useful at accurately predicting the presence of linear Type A and concentric Type B cracks in remote sensing images, implying that these two classifications might prove useful in other remote sensing environments at saying whether or not observed features are the result of inflation of pahoehoe lava flows, such as near Phlegra in the Elysium Volcanic Province on Mars. Further field work on the McCartys Flow could also be undertaken to more closely examine certain aspects of the cracks that would provide more evidence to support the contention that they were formed during inflation. For example, looking at the banding and layering with certain cracks to determine consistency with similar observations made in other studies (Hon et al. 1994; Hoblitt et al. 2012) would be a possible strategy, as well as categorizing individual cracks using the crack classification model to see if any trends would emerge within a large set. Crack width and

depth analysis on the flow to the north or south of the Lava Falls area would also provide more data for looking at the emplacement model suggested to account for the inflation of the McCartys Flow, particularly if a lack of a linear trend in crack widths compared to crack depths could be shown across other parts of the flow, particularly on distinctly separate plateau areas. Further mapping of the McCartys Flow to determine where individual plateau levels begin and end, combined with extensive field observations and possible DGPS surveying would be a possible approach for accumulating more data to support the proposed model of inflation.

The DGPS elevation profiles and analysis of the plateau near Lava Falls confirmed based on methods developed by Walker (1991) and Hon et al. (1994) that the McCartys Flow is likely an inflated pahoehoe sheet flow. While analysis of the end members of the transects was less conclusive because of the inability to see the extent the plateau crust extended below ground, analysis of the two major transects that crossed the flow (Transects G and K) provided evidence of uniform uplift and characterization of the McCartys Flow as a sheet flow. In terms of emplacement history, analysis of the crack widths versus crack depths across the flow did not produce a linear pattern that would suggest constant inflation. The proposed emplacement model of successive plateaus may be supported by this conclusion, however, further field work and analysis of a larger region of the McCartys Flow would be required to say whether the plateau model of emplacement is valid or not. For example, any depressions located further north on the flow but still south of the vent could be analyzed using a DGPS unit and their profiles and elevations compared to the depressions on the part of the flow already investigated. If the depression bottom elevations at these topographically higher areas are higher than those on the theoretically topographically lower Lava Falls area, this would be a good indicator that the

proposed emplacement model might be a good explanation of the McCartys Flow emplacement history.

References

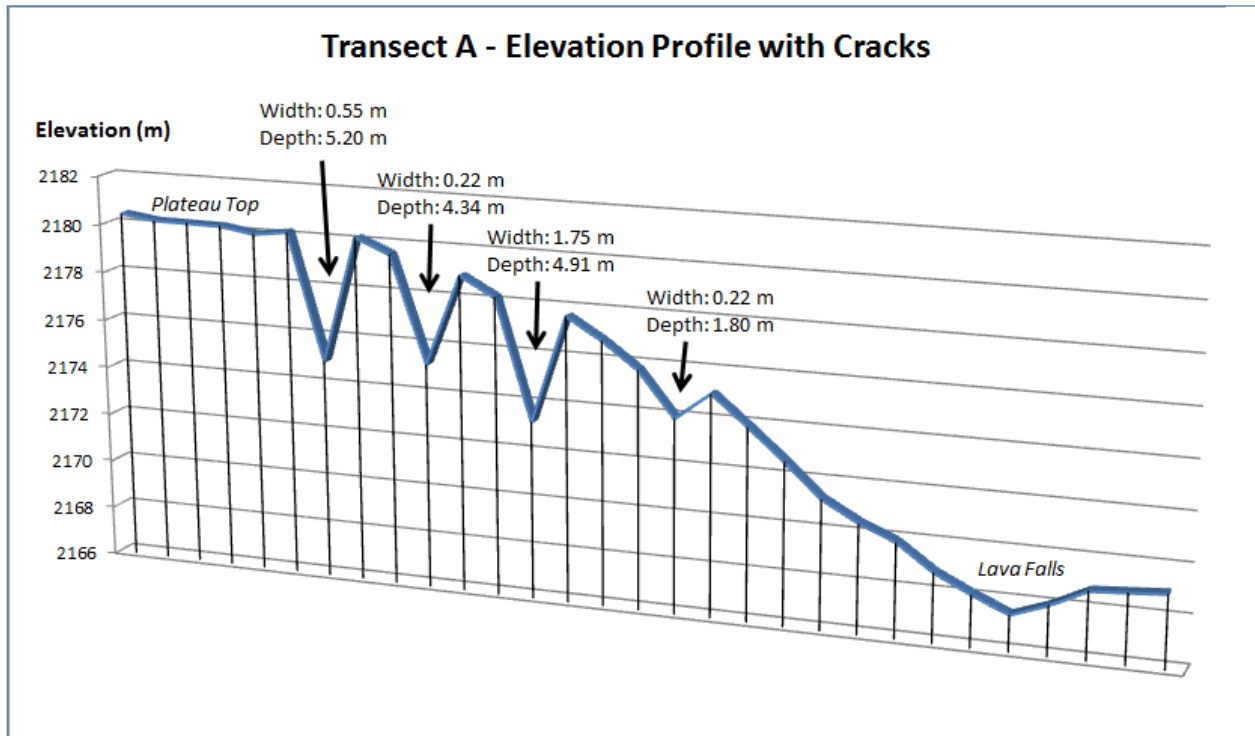
- Dunbar, N. W. and Phillips, F. M., 2004, Cosmogenic ^{36}Cl ages of lava flows in the Zuni-Bandera volcanic field, north-central New Mexico, U.S.A.: New Mexico Bureau of Geology & Mineral Resources Bulletin 160, pp. 309-317.
- Fink, J. H. and Fletcher, R. C., 1978, Ropey pahoehoe: surface folding of a viscous fluid: *Journal of Volcanology and Geothermal Research*, v. 4, pp. 151-170.
- Hamilton, C. W., 2013, Flood lavas associated with the Cerberus Fossae 2 unit in Elysium Planitia, Mars: Lunar and Planetary Science Institute, 44th Lunar and Planetary Science Conference (2013), no. 3070.
- Hoblitt, R. P., Orr, T. R., Heliker, C., Denlinger, R. P., Hon, K. A., and Cervelli, P. F., 2012, Inflation rates, rifts, and bands in a pahoehoe sheet flow: *Geosphere*, v. 08, no. 1, pp. 179-195.
- Hon, K. A., Gansecki, C., Kauahikaua, J. P., 2003, The transition from 'a'a to pahoehoe crust on flows emplaced during the Pu'u 'O'o-Kupaianaha eruption, chap. 5 of Heliker, C., Swanson, D. A., and Takahashi, T. J., eds., *The Pu'u 'O'o-Kupaianaha Eruption of Kilauea Volcano, Hawai'i: The First 20 Years*: U.S. Geological Survey Professional Paper 1676, pp. 89-104.
- Hon, K. A., Kauahikaua, J. P., Denlinger, R. P., and Mackay, K., 1994, Emplacement and inflation of pahoehoe sheet flows: Observations and measurements of active lava flows on Kilauea Volcano, Hawaii: *Geological Society of America, Bulletin*, v. 106, pp. 351-370.

- Keszthelyi, L. P., 2013, A facies model for primary mafic volcanic deposits: Lunar and Planetary Science Institute, 44th Lunar and Planetary Science Conference (2013), no. 2567.
- Laughlin, A., Aldrich, M., Ander, M., Heiken, G., and Vaniman, D., 1982, Tectonic setting and history of late-Cenozoic volcanism in west-central New Mexico: New Mexico Geological Society Guidebook, v. 33, pp. 279-284.
- Laughlin, A. W., Charles, R. W., Reid, K., and White, C., 1993, Field trip guide to the geochronology of El Malpais National Monument and the Zuni-Bandera volcanic field, New Mexico: New Mexico Bureau of Mines & Mineral Resources Bulletin 149, New Mexico Institute of Mining & Technology.
- Laughlin, A. W., Manzer, G. K. Jr., and Carden, J. R., 1974, Feldspar megacrysts in alkali basalts: Geological Society of America, Bulletin, v. 85, pp. 413-416.
- Mabery, M. V., Moore, R. B., and Hon, K. A., 1999, The volcanic eruptions of El Malpais: a guide to the volcanic history and formations of El Malpais National Monument: Ancient City Press, Santa Fe, New Mexico, USA, pp. 44-48.
- Platz, T. and Michael, G. G., 2011, Eruption history of the Elysium Volcanic Province, Mars: Earth and Planetary Science Letters 312, pp. 140-151.
- Scheidt, S. P., Hamilton, C. W., Zimbelman, J. R., Bleacher, J. E., Garry, W. B., de Wet, A. P., and Crumpler, L. S., Lava-rise plateaus and inflation pits within the McCartys Lava Flow, New Mexico, USA: Lunar and Planetary Science Institute, 45th Lunar and Planetary Science Conference (2014), no. 1491.
- Schmincke, H., 2004, Volcanism: Springer-Verlag, Berlin, Germany, p. 23.

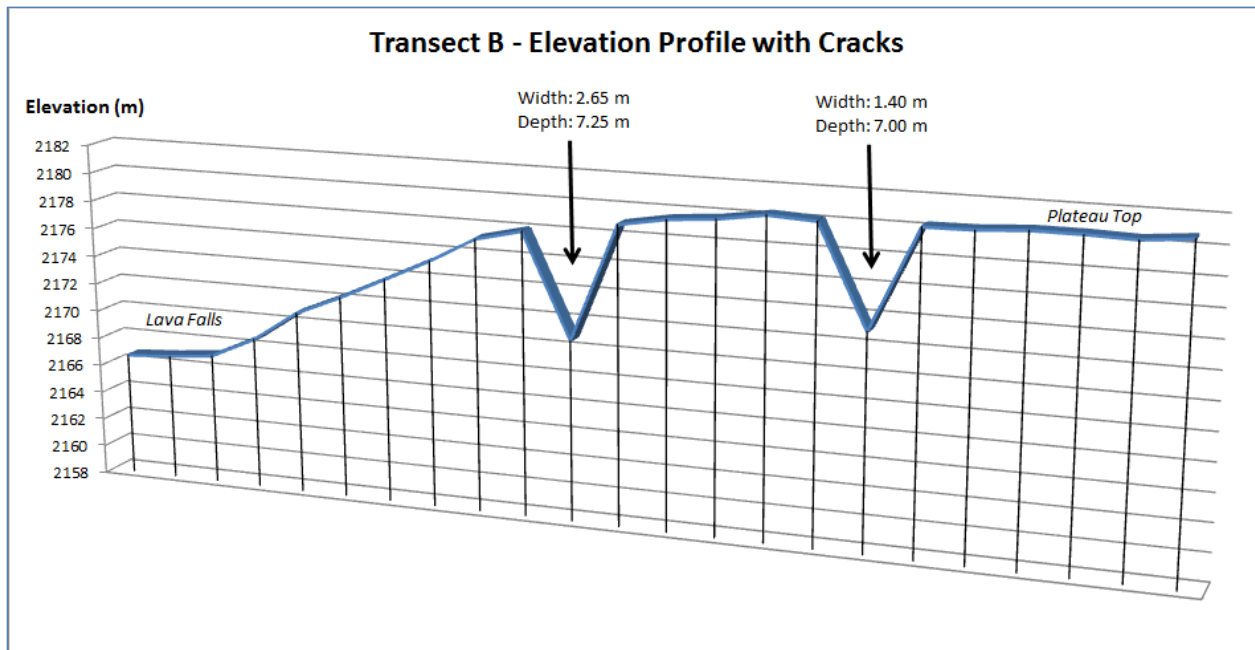
Self, S., Keszthelyi, L. P., and Thordarson, T., 1998, The importance of pahoehoe: Annual Review of Earth and Planetary Science, no. 26, pp. 81-110.

Walker, G. P. L. 1991. Structure and origin by injection of lava under surface crust, of tumuli, "lava rises", "lava-rise pits", and "lava-inflation clefts" in Hawaii. Bulletin of Volcanology, 53; pp. 546-558.

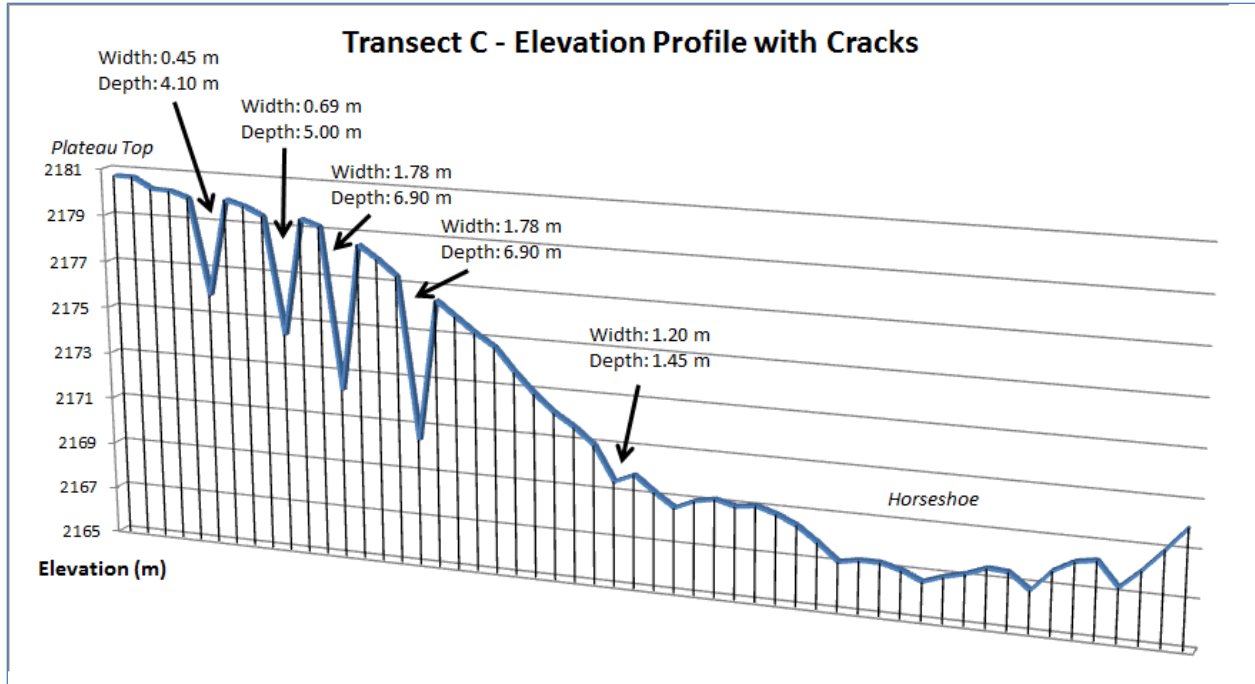
Appendix



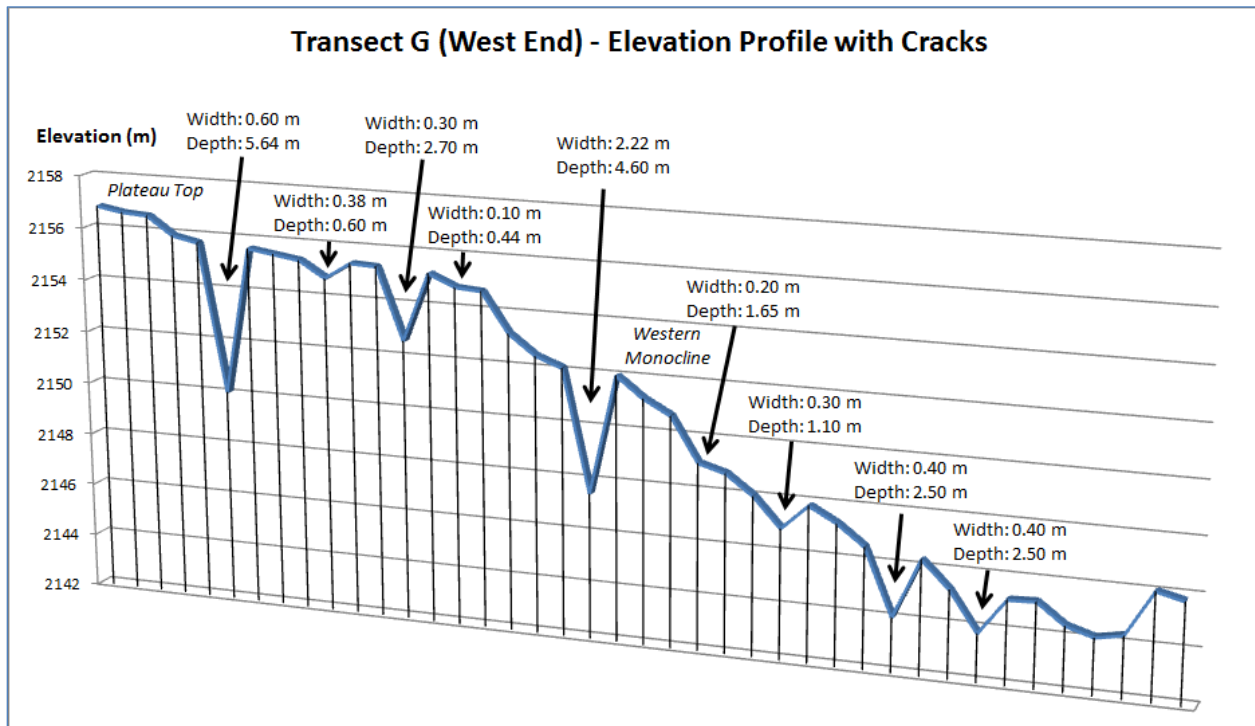
i) - Elevation profile and crack depths of Transect A.



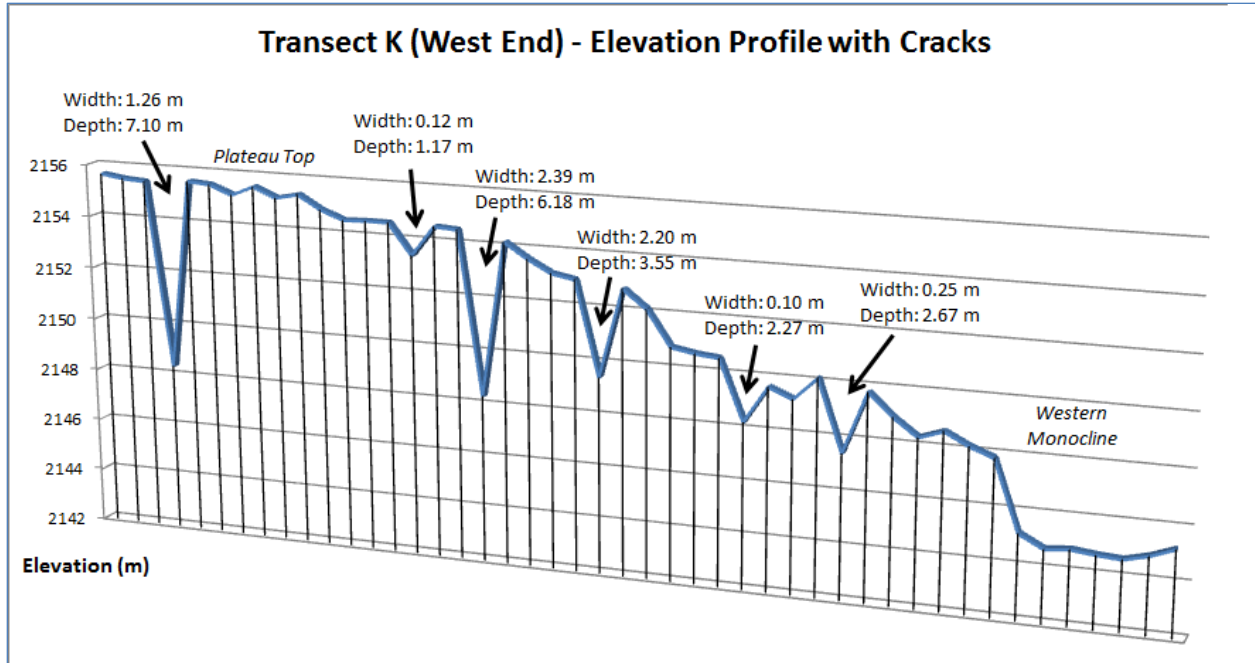
ii) - Elevation profile and crack depths of Transect B.



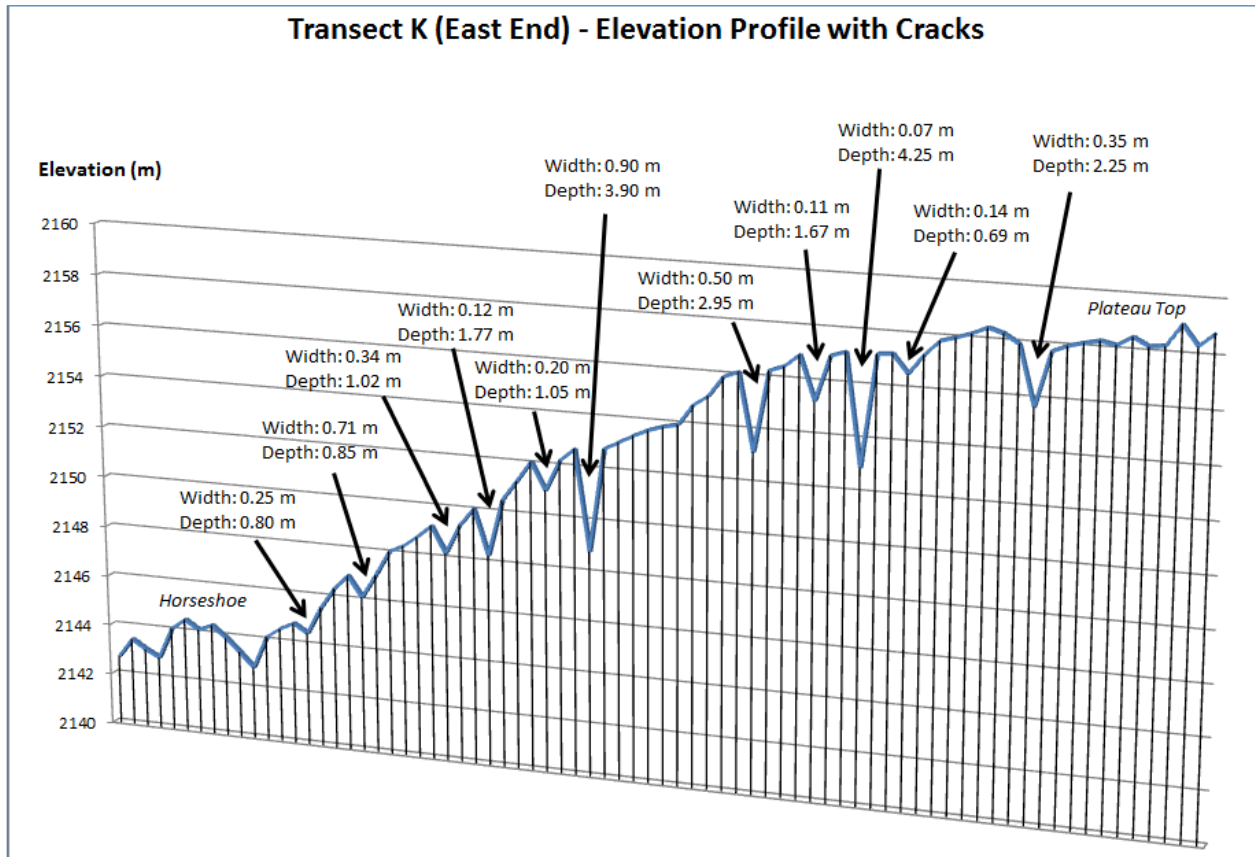
iii) - Elevation profile and crack depths of Transect C.



iv) - Elevation profile and crack depths of the west end member of Transect G.



v) - Elevation profile and crack depths of west end member of Transect K.



vi) - Elevation profile and crack depths of the east end of Transect K.